

Chulalongkorn University

Chula Digital Collections

Chulalongkorn University Theses and Dissertations (Chula ETD)

2022

Classification of bacteria and fungi in peritoneal dialysis fluids of patients with chronic kidney disease based on metagenomic analysis

Suthida Visedthorn
Faculty of Medicine

Follow this and additional works at: <https://digital.car.chula.ac.th/chulaetd>



Part of the [Medical Biochemistry Commons](#)

Recommended Citation

Visedthorn, Suthida, "Classification of bacteria and fungi in peritoneal dialysis fluids of patients with chronic kidney disease based on metagenomic analysis" (2022). *Chulalongkorn University Theses and Dissertations (Chula ETD)*. 5938.

<https://digital.car.chula.ac.th/chulaetd/5938>

This Thesis is brought to you for free and open access by Chula Digital Collections. It has been accepted for inclusion in Chulalongkorn University Theses and Dissertations (Chula ETD) by an authorized administrator of Chula Digital Collections. For more information, please contact ChulaDC@car.chula.ac.th.

Classification of Bacteria and Fungi in Peritoneal Dialysis
Fluids of Patients with Chronic Kidney Disease Based on
Metagenomic Analysis

Miss Suthida Visedthorn



A Thesis Submitted in Partial Fulfillment of the Requirements
for the Degree of Master of Science in Medical Biochemistry
Department of Biochemistry
FACULTY OF MEDICINE
Chulalongkorn University
Academic Year 2022
Copyright of Chulalongkorn University

การจำแนกแบคทีเรียและราที่พบในน้ำยาล้างไตทางช่องท้องของผู้ป่วยโรคไตเรื้อรังโดยอาศัยการ
วิเคราะห์ทางเมตาจีโนม



วิทยานิพนธ์นี้เป็นส่วนหนึ่งของการศึกษาตามหลักสูตรปริญญาวิทยาศาสตรมหาบัณฑิต
สาขาวิชาชีวเคมีทางการแพทย์ ภาควิชาชีวเคมี
คณะแพทยศาสตร์ จุฬาลงกรณ์มหาวิทยาลัย
ปีการศึกษา 2565
ลิขสิทธิ์ของจุฬาลงกรณ์มหาวิทยาลัย

Thesis Title	Classification of Bacteria and Fungi in Peritoneal Dialysis Fluids of Patients with Chronic Kidney Disease Based on Metagenomic Analysis
By	Miss Suthida Visedthorn
Field of Study	Medical Biochemistry
Thesis Advisor	SUNCHAI PAYUNGORN
Thesis Co Advisor	TALERNGSAK KANJANABUCH

Accepted by the FACULTY OF MEDICINE,
Chulalongkorn University in Partial Fulfillment of the
Requirement for the Master of Science

..... Dean of the FACULTY
OF MEDICINE
(CHANCHAI SITTIPUNT)

THESIS COMMITTEE

..... Chairman
(Sittisak Honsawek)

..... Thesis Advisor
(SUNCHAI PAYUNGORN)

..... Thesis Co-Advisor
(TALERNGSAK KANJANABUCH)

..... Examiner
(PORNCHEI KAEWSAPSAK)

..... External Examiner
(Piyada Linsuwanon)

สุธิดา วิเศษธร : การจำแนกแบคทีเรียและราที่พบในน้ำยาล้างไตทางช่องท้องของผู้ป่วยโรคไตเรื้อรังโดยอาศัยการวิเคราะห์ทางเมตาจีโนม. (Classification of Bacteria and Fungi in Peritoneal Dialysis Fluids of Patients with Chronic Kidney Disease Based on Metagenomic Analysis)
 อ.ที่ปรึกษาหลัก : ศัญชัย พงษ์กร, อ.ที่ปรึกษาร่วม : เถลิงศักดิ์ กาญจนบุษย์

โรคไตเรื้อรัง (Chronic kidney disease: CKD) คือ สภาวะที่ไตถูกทำลายอย่างต่อเนื่องเป็นระยะเวลานาน ซึ่งนำไปสู่การเสื่อมสภาพการทำงานของไตอย่างเรื้อรัง หรือที่เรียกว่าโรคไตเรื้อรังระยะสุดท้าย (End-stage kidney disease: ESKD) โดยมีวิธีการบำบัดทดแทนไตด้วยการล้างไตทางช่องท้อง (Peritoneal dialysis: PD) ซึ่งเป็นวิธีที่สามารถปรับปรุงคุณภาพชีวิตของผู้ป่วยได้อย่างมีประสิทธิภาพ อย่างไรก็ตาม ภาวะเยื่อช่องท้องอักเสบ (Peritonitis) ยังคงเป็นภาวะแทรกซ้อนที่สำคัญจากการบำบัดทดแทนไตที่อาจนำไปสู่การเสียชีวิต และการตรวจหาเชื้อก่อโรคหรือเชื้อที่เกี่ยวข้องกับภาวะแทรกซ้อนนี้ ยังคงให้ผลลัพธ์เป็นลบในอัตราที่สูง ในงานวิจัยนี้มีวัตถุประสงค์เพื่อศึกษาทางด้านเมตาจีโนมิกส์ด้วยวิธีการหาลำดับนิวคลีโอไทด์แบบนาโนพอร์จากตัวอย่างน้ำยาล้างไตทางช่องท้อง (Peritoneal dialysis effluent: PDE) ของผู้ป่วยโรคไตเรื้อรัง โดยการหาลำดับนิวคลีโอไทด์ของยีน 16S บนไรโบโซมอลดีเอ็นเอ (16S rDNA) และบริเวณ Internal transcribe spacer (ITS) สำหรับการระบุชนิดแบคทีเรียและเชื้อราตามลำดับ จากผลการศึกษา พบว่าสามารถจำแนกแบคทีเรียได้จนถึงระดับสปีชีส์ ได้แก่ *Escherichia coli*, *Phyllobacterium myrsinacearum*, *Streptococcus gallolyticus*, *Staphylococcus epidermidis* และ *Shewanella algae* ตามลำดับ ในขณะที่พบเชื้อราในสกุล *Wallemia* จากตัวอย่างน้ำยาล้างไตทางช่องท้องมากที่สุด จากผลการศึกษานี้สามารถสรุปได้ว่าวิธีการทางเมตาจีโนมิกส์ข้างต้น มีประสิทธิภาพในการระบุชนิดแบคทีเรียและเชื้อราได้ดีกว่าวิธีการแบบดั้งเดิม ซึ่งเป็นอีกหนึ่งทางเลือกในการจำแนกสิ่งมีชีวิตด้วยวิธีการที่ไม่อาศัยการเพาะเชื้อ เพื่อเป็นแนวทางการรักษาและป้องกันสำหรับผู้ป่วยโรคไตเรื้อรังในอนาคต

สาขาวิชา ชีวเคมีทางการแพทย์

ลายมือชื่อนิสิต

ปีการศึกษา 2565

ลายมือชื่อ อ.ที่ปรึกษาหลัก

ลายมือชื่อ อ.ที่ปรึกษาร่วม

6370109130 : MAJOR MEDICAL BIOCHEMISTRY

KEYWORD Bacteria, Chronic kidney disease, Fungi, Metagenomic
RD: sequencing, Peritoneal dialysis

Suthida Visedthorn : Classification of Bacteria and Fungi in
Peritoneal Dialysis Fluids of Patients with Chronic Kidney
Disease Based on Metagenomic Analysis. Advisor: SUNCHAI
PAYUNGORN Co-advisor: TALERNGSAK
KANJANABUCH

Chronic kidney disease (CKD) is a long-term condition where sustained damage of the renal parenchyma leads to the chronic deterioration of renal function that may gradually progress to end-stage kidney disease (ESKD). Peritoneal dialysis (PD) is a type of ESKD treatment that is beneficial to improve a patient's quality of life. However, PD-associated peritonitis is a major complication that contributes cause of death, and the detection of the pathogen provided a high culture-negative rate. This study aims to apply metagenomic approaches for identifying the bacteria and fungi in peritoneal dialysis effluent (PDE) of CKD patients based on the full-length 16S ribosomal DNA (rDNA) gene and Internal transcribe spacer (ITS) region, respectively. As a result, the five major bacteria species, including *Escherichia coli*, *Phyllobacterium myrsinacearum*, *Streptococcus gallolyticus*, *Staphylococcus epidermidis*, and *Shewanella* algae were observed in PDF samples, whereas the most fungal genera in PDE samples was *Wallemia*. The results suggested that our metagenomic approach provided a high potential for bacterial and fungal taxonomic identification than the traditional culture method, which would be a practical and alternative culture-independent approach and offers a preventive infectious strategy in CDK patients.

Field of Study:	Medical Biochemistry	Student's Signature
Academic Year:	2022
		Advisor's Signature
	
		Co-advisor's Signature
	

ACKNOWLEDGEMENTS

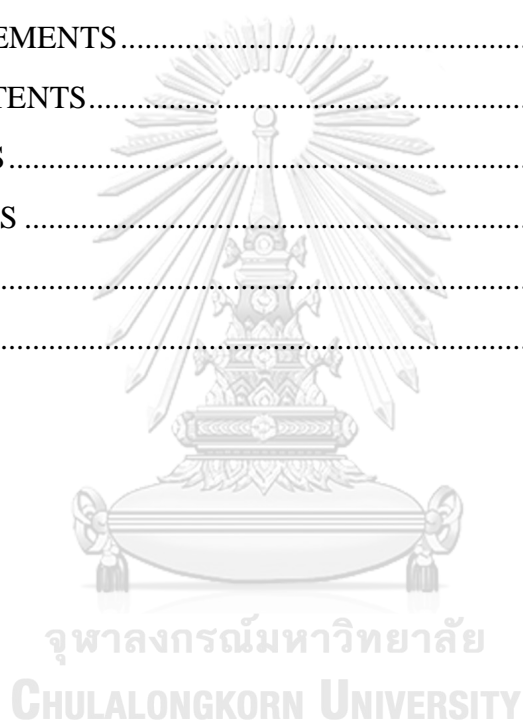
I would like to acknowledge my advisor, Prof. Sunchai Payungporn, Ph.D., and my co-advisor, Prof. Talerngsak Kanjanabuch, M.D., for individual giving support, worthy guidance, and knowledge through all the stages of my master's research. I also would like to thank all researchers from the Center of Excellence in Kidney Metabolic Disorders, Chulalongkorn University, for supporting sample processing in CKD patients. Moreover, I am indebted to all members of the Center of Excellence in Systems Microbiology (CESM), Chulalongkorn University, for technical support, valuable suggestions, and assistance for the experiment of this study, which have significantly contributed to the development of my research work.

Furthermore, I would like to acknowledge the tuition and financial support received from the H.M. the King Bhumibhol Adulyadej 72nd Birthday Anniversary Scholarship. This study also received a grant from the Ratchadapisek Sompot Fund [GA66/19], Faculty of Medicine, Chulalongkorn University, and the National Research Council of Thailand (NRCT). Their funding has been crucial in enabling me to pursue my master's degree studies and conduct my research effectively.

Suthida Visedthorn

TABLE OF CONTENTS

	Page
.....	iii
ABSTRACT (THAI)	iii
.....	iv
ABSTRACT (ENGLISH)	iv
ACKNOWLEDGEMENTS	v
TABLE OF CONTENTS	vi
LIST OF TABLES	vii
LIST OF FIGURES	viii
REFERENCES	58
VITA	66



LIST OF TABLES

	Page
Table 1: The correlation between age and average eGFR level in healthy adults	14
Table 2: Taxonomic identification methods comparisons	17
Table 3: Primers used for 16S rDNA and ITS amplifications	29
Table 4: PCR reaction components for 16S rDNA amplification	30
Table 5: Thermal cycling for 16S rDNA amplification.....	30
Table 6: PCR reaction components for ITS amplification.....	31
Table 7: Thermal cycling for ITS amplification	31
Table 8: Summary of 16S rDNA sequencing data.....	36
Table 9: Alpha diversity indexes (Chao1 and Shannon) of bacteria	37
Table 10: Summary of concordant bacterial species in both methods.....	43
Table 11: Summary of different bacterial species between the metagenomic approach and traditional culture method	44
Table 12: Summary of bacterial species through the only metagenomic method	45
Table 13: Summary of ITS2 sequencing data.....	47
Table 14: Alpha diversity indexes (Chao1 and Shannon) of fungi.....	48
Table 15: Summary of fungal identification through the metagenomic approaches ...	53
Table 16: The comparison of positive rate from bacterial culture and metagenomic analysis between our study and recent report	55

LIST OF FIGURES

	Page
Figure 1: The stages of CKD, GFR levels, and percentage of kidney function	14
Figure 2: The procedure for peritoneal dialysis	16
Figure 3: The schematic of ribosome complex and 16S rDNA gene	19
Figure 4: The schematic of the rDNA genes in eukaryotes	20
Figure 5: The schema of a DNA molecule translocating a protein nanopore.....	23
Figure 6: The schema of the nanopore sequencing system.....	23
Figure 7: The Overview of the nanopore sequencing process using MinION	24
Figure 8: The summary of new chemistry, kit 14.....	24
Figure 9: Research workflow of metagenomic analysis based on amplicon sequencing from PDE samples	25
Figure 10: Data analysis workflow of metagenomic analysis based on amplicon sequencing from PDE samples	32
Figure 11: The 1% agarose gel electrophoresis for comparisons among 3 primer pairs specific to bacterial 16S rDNA PCR products.....	35
Figure 12: The representative PCR products obtained from the amplification of the 16S rDNA gene using 16S_27F/16S_806R primers	35
Figure 13: Rarefaction curve analysis of 16S rDNA gene	36
Figure 14: The taxonomic composition of bacterial classification in 89 PDE samples	38
Figure 15: The relative abundance (%) of 55 bacteria at the genus level.....	39
Figure 16: The relative abundance (%) of 84 bacteria at the species level.....	40
Figure 17: Heatmap visualized the hierarchical clustering of the bacterial community of each sample based on the analysis of the 35 most abundant species	41
Figure 18: Venn diagram illustrated the number of PDE samples that can be classified for bacterial species based on the metagenomic approach (V1-V4) and traditional culture method	42
Figure 19: The 1% agarose gel electrophoresis for comparisons among 3 primer pairs specific to fungal ITS PCR products	46

Figure 20: The representative PCR products obtained from the amplification of fungal ITS2 by ITS2_86F/ITS_4R primers	47
Figure 21: The rarefaction analysis of ITS2	48
Figure 22: The taxonomic classification of fungal phyla in 69 PDE samples.....	49
Figure 23: The taxonomic classification of fungal genera in 69 PDE samples	50
Figure 24: Heatmap visualized the hierarchical clustering of the fungal taxonomy in each sample based on genus level.....	51



CHAPTER 1

INTRODUCTION

Rationale

Chronic kidney disease (CKD) is a long-term condition where sustained damage of the renal parenchyma leads to the chronic deterioration of renal function that may gradually progress to end-stage kidney disease (ESKD) (1). ESKD remains regularly fatal without kidney replacement therapy such as dialysis and kidney transplant. Peritoneal dialysis (PD) is a type of dialysis that uses the peritoneum in the patient's abdomen as the membrane through dialysate by which fluid and dissolved substances are exchanged with the blood. The excess fluid, toxins, and other substances as consequences of kidney failures are also removed through this process (2). PD is beneficial because it can be done at home, with no need to drive to a hospital, is more cost-effective, reduced dietary restrictions, increased freedom perception and patient satisfaction, and possibly improved quality of life (3). Unfortunately, PD remains a certain high risk of infection of the peritoneum, subcutaneous tunnel and catheter exit site. Even though this dialysis technique is one of the promising methods, it might increase the potential of microbial contamination in the blood through the catheter which compromises the immune defense system of patients leading to complications, morbidity, and mortality (3, 4).

The most recognized factor associated with PD patients' peritonitis is contamination through an exogenous route with skin pathogenic bacteria, *Staphylococcus*, which might occur during connection and disconnection of the dialysis transfer-set (5, 6). The endogenous contamination route of the peritoneal cavity, including the hematogenous route, and translocation of microorganisms through the intestinal epithelial barrier, affects the structural and functional occurs, thereby facilitating the translocation of intestinal microorganisms, endotoxins, antigens, and other microbial products through the intestinal wall toward the systemic circulation and the internal milieu (5, 7, 8, 9).

Nowadays, metagenomic next-generation sequencing (mNGS) is a promising alternative approach for broad-spectrum microbial identification in clinical samples,

as this approach allows for the unbiased detection of nearly all potential microbial, including bacteria, fungi, viruses, and parasites. This approach can use to overcome the limitations of the traditional methods, which can be detected by uniquely identifying DNA or RNA shotgun sequences (10). This method has been successfully applied for the clinical diagnosis of infectious diseases (11), outbreak response, and pathogen discovery (10, 12). In particular, purulent fluids, often suggest an infectious etiology, which can decrease assay sensitivity (13). Most metagenomic studies have employed Illumina sequencing platforms, with sequencing run times exceeding 16 hours and overall sample-to-answer turnaround times of 48–72 hours. In contrast with Illumina sequencing, Oxford Nanopore Technologies (ONT) is a third-generation sequencing technology that has two key advantages over second-generation technology in longer reads and the ability to perform real-time sequence analysis and actionable information, allowing detection of the potential microbial within minutes after the sequencing and requiring less turnaround time of fewer than 6 hours (13, 14).

However, the microbial contamination that may influence the occurrence of infection remains unclearly classified and this knowledge gap is urgently needed to be filled. This study aims to classify the bacteria and fungi from peritoneal dialysis effluent (PDE) that might serve as a cause for high morbidity and mortality of CKD patients by utilizing 16S rDNA and ITS region through the next-generation sequencing approaches. Furthermore, the information on bacterial and fungal profiles of CKD patients will be compared to the specificity or accuracy by using a culture-dependent method which is the gold standard method for bacterial and fungal species identification and used to develop the rapid diagnosis pipeline at the early phase of infection.

Objectives

To identify the bacteria and fungi in peritoneal dialysis effluent of chronic kidney disease patients through metagenomic approaches.

Research question

Can bacteria and fungi in peritoneal dialysis effluent of CKD patients be examined and identified through metagenomic approaches?

Hypothesis

The bacteria and fungi in peritoneal dialysis effluent can be identified and examined through metagenomic approaches.

Keywords

bacteria; chronic kidney disease; fungi; metagenomic sequencing; peritoneal dialysis



CHAPTER II

LITERATURE REVIEW

1. Chronic kidney disease

Chronic kidney disease (CKD) is a condition in which the kidneys are unable to clear waste products, it affects an estimated 10% of the global population or 700 million people are at risk (15). CKD is a global public health problem that is increasingly recognized in the present day (16). It is associated with high morbidity and, in the advanced stage, requires life-support treatment by renal dialysis or transplantation (17). There are multiple risk factors for progressing kidney diseases such as diabetes, high blood pressure, heart disease, and a family history of kidney failure (18). CKD has occurred without any signs and symptoms that can be used for disease prediction. The process occurs at a slow rate and leads to the development of kidney damage over time. Loss of kidney function can cause fluid or waste product build-up, which cannot eliminate from the body. Depending on the severity of the CKD, loss of kidney function can cause symptoms such as nausea, vomiting, urinating more or less, sleep problems, and chest pain if fluid builds up around the lining of the heart, or high blood pressure (hypertension) which is an uncontrollable condition that leads to symptoms (19).

CKD can be divided into 5 stages based on the Estimated Glomerular Filtration Rate (eGFR) test result, which refers to how well the kidneys can filter waste and extra fluid out of the blood (20). GFR is an important and highly accurate estimate for identifying kidney disease progression, which is the standard way to estimate from a blood test for measuring creatinine levels. Creatinine is a waste product from muscle tissue's normal breakdown and digestion of dietary protein. In healthy adults, the normal eGFR level is greater than 90 and it declines with age despite no kidney failure. See the chart in Table 1 for the average estimated eGFR based on age (21).

Table 1: The correlation between age and average eGFR level in healthy adults

Age (years)	Average eGFR
20 – 29	116
30 – 39	107
40 – 49	99
50 – 59	93
60 – 69	85
70+	75

In the early stages (Stages 1–3), kidney disease doesn't usually cause symptoms and it is still able to filter waste out of the blood. In the later stages (Stages 4–5), CKD causes symptoms since the kidneys must work harder to filter the blood and may stop working eventually (20, 21). The stages of CKD, GFR levels, and percentage of kidney function in each stage are shown in Figure 1.

STAGES OF CHRONIC KIDNEY DISEASE	GFR*	% OF KIDNEY FUNCTION
Stage 1 Kidney damage with normal kidney function	90 or higher	90–100%
Stage 2 Kidney damage with mild loss of kidney function	89 to 60	89–60%
Stage 3a Mild to moderate loss of kidney function	59 to 45	59–45%
Stage 3b Moderate to severe loss of kidney function	44 to 30	44–30%
Stage 4 Severe loss of kidney function	29 to 15	29–15%
Stage 5 Kidney failure	Less than 15	Less than 15%

* Your GFR number tells you how much kidney function you have. As kidney disease gets worse, the GFR number goes down.

Figure 1: The stages of CKD, GFR levels, and percentage of kidney function

There are 5 stages of CKD progression divided by eGFR levels. Kidney disease can get worse in time. In the early stages (Stages 1-3), kidneys are still able to filter waste out of blood. In the later stages (Stages 4-5), kidneys must work harder to filter blood and may stop working altogether (21).

Once the kidneys have failed, the patient will need to start dialysis or has a kidney transplant. Dialysis helps clean the blood when the kidneys have failed. There are 2 types of dialysis including hemodialysis and peritoneal dialysis. A kidney transplant is a surgery, which replaces the non-functional kidney with a healthy kidney from a donor. (21, 22)

2. Peritoneal dialysis

Peritoneal dialysis (PD) is an attractive treatment option, among other kidney dialyzes, for end-stage kidney disease (ESKD) patients wishing for increased treatment-related flexibility and autonomy (23).

For PD, the blood is cleaned inside the body, the abdominal cavity, or the hollow space that surrounds the organ in the patient's abdomen. The lining of the abdominal cavity, or peritoneum, is well-supplied with blood and covers the organs such as the small and large intestines thereby it appropriately serves as a semipermeable membrane for dialysis. Before starting the treatment, a catheter has to be inserted into the abdominal cavity whereof allows the dialysis fluid into the peritoneal cycle by itself. Any toxicity and harmful substances from the blood vessels will diffuse into the dialysis fluid. A lot of substances similar to sugar and electrolytes and excess water are removed from the blood by osmosis. After a few hours, the dialysis fluid has to be drained from the abdominal cavity newly and is usually replaced with fresh dialysis fluid immediately. Thus, the blood is constantly being cleaned. In addition, a cycler is an automatic device for more comfortably draining and replacing the dialysis fluid at night (24). In the process of peritoneal dialysis, the dialysis fluid is passed into the abdominal cavity as shown in Figure 2.

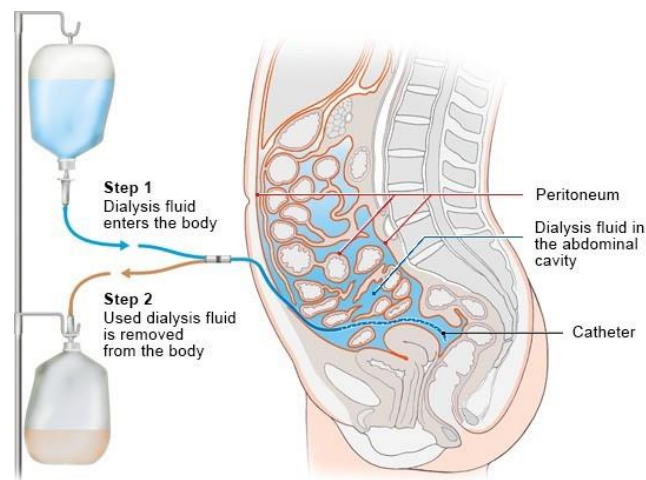


Figure 2: The procedure for peritoneal dialysis

The first step is the process of draining the used and saturated solution inside the abdomen via the catheter. After the abdomen is drained of the used solution, the peritoneal cavity is refilled with new dialysis fluid solution through the same catheter. Next step, during this dwell period, the dialysis solution stays in the peritoneal cavity. This is when and where the dialysis occurs. The solution in your peritoneal cavity is collecting the waste and excess fluid from your body (24).

Although PD is suggested as an effective treatment modality for ESKD patients, peritonitis remains a major complication that might result in the discontinuation of the treatment (25). If the patient does not concern about cleanliness, it may lead to infection of the peritoneum, subcutaneous tunnel, and catheter exit site (4).

Previous studies have shown that patients who perform PD experience superior satisfaction and better preservation of kidney function (26, 27, 28, 29). Additionally, PD can be done at home. There is no need to drive to a hemodialysis center, and it is more cost-effective. Also, it reduces dietary restrictions and has less hemodynamically instability during hemodialysis. Hence, overall it improves the quality of life (3).

3. Metagenomics sequencing

The accurate identification of the pathogen disease is crucial for the correct diagnosis and treatment of the infection. A comprehensive, accurate, and rapid diagnosis, including pathogen identification at the species level and antibiotic resistance pattern, enables physicians to use more targeted antimicrobial therapies for these patients (30). Presently, many methods can be used to characterize the microbial composition and identify the potential causative from an infected patient's sample such as microbial culture, polymerase chain reaction (PCR) and high-throughput sequencing (HTS) (31). The identification methods comparisons are shown in Table2.

Table 2: Taxonomic identification methods comparisons

Technique	Speed (days)	Accuracy	Resistance mutations	Multispecies	High throughput	Emergent pathogen
Culture	2-14	Genus or Species	No	No	No	No
PCR	2	Genus or Species	No	No	No	No
Amplicon sequencing	1.5-2	Genus or Species	No	Yes	Yes	Yes
Shotgun sequencing	2-3	Species or Strain	Yes	Yes	Yes	Yes

Microbial culture has been considered the gold standard of diagnostic methods developed more than 100 years ago. It involves growing the pathogen on appropriate media for bacterial and fungal species and is widely used in clinical laboratories (30). Further identification of the pathogen after culture specifically at the species level, biochemical and additional testing such as antibiotic resistance tests are often required. Due to the limitations of the media utilized for growth, there will be inherent bias to cultures. Moreover, this technique can only verify the presence of a microorganism that can grow on the selected media. Accordingly, a culture technique might not be effective at identifying unculturable, unknown, or novel pathogens (30).

PCR assays are rapid, low-cost, and specific on the short possible target list. The weakness of this technique as a diagnostic tool is its potential bias because the primer sequences target has to be chosen and designed before testing. In addition, PCR has relatively low-throughput capabilities because multiple PCR amplifications per sample negatively affect cost and time effectiveness (32).

For amplicon-based metagenomic sequencing, the approach uses PCR to create sequences of DNA called amplicons. It is a widely used technique that relies on the conserved and variable. Amplicons from different samples can be multiplexed, which involves adding a barcode to samples, which can later be identified. The individual samples used for amplicon sequencing, typically used for variant detection, have to be transformed into libraries by adding adapters before multiplexing. Those adapters are allowing the amplicons to adhere to the flow cell for sequencing, and add enriching target regions via PCR amplification (33). 16S rDNA gene sequencing target is only read a region of the 16S rDNA gene which is found in all Bacteria and Archaea can only identify these types of microorganisms. Other types of amplicon sequencing such as ITS sequencing for fungi or 18S sequencing for protists, can identify other microorganisms. HTS technologies have constantly improved, and the overall quality read length of the sequencing has also improved which allows for greater and specific species resolution (34).

Shotgun metagenomic sequencing involves randomly breaking DNA into many small pieces, much like a shotgun would break something up into many pieces. These DNA fragments are then sequenced and combined through bioinformatics tools to identify the genes and species in the sample. Unlike 16S rDNA sequencing, shotgun metagenomic sequencing can read all genomic DNA in a sample, rather than just one specific region of DNA (35). This method is culture independence and avoids PCR bias and it is not restricted to only bacterial sequence (31, 36). In addition, the coverage of the genome outside of the small 16S rDNA gene region means that specific, strain-level discrimination is achievable. Shotgun sequencing captures not only the pathogenic sequences but also the human host's genetic material, which can overwhelm the signal from the pathogens and lead to inaccurate classification of the pathogenic community. On the other hand, human genetic sequences can be expedient

in examining a genetic response to pathogen infection. Therefore, for fully integrated into diagnostic protocols, the relative benefits should be compared and validated by using culture methods (31, 37, 38, 39).

4. 16S ribosomal DNA gene

The ribosome is a complex of plural proteins and DNA subunits found within all living cells, that play an important role in biological protein synthesis (translation). The ribosome is composed of two major components: the small ribosomal subunit (30S ribosomal subunit in prokaryotic cells), and the large subunit (50S ribosomal subunit in prokaryotic cells) (40). The 16s ribosomal DNA (16S rDNA) gene encodes a ribosomal DNA molecule of 30S ribosomal subunit present in all prokaryotic cells, including bacteria and archaea that was the phylogenetic marker of choice from an early stage and has been used extensively to date (40, 41). The 16S rDNA gene is commonly and widely used for identifying bacteria for several reasons. First, the gene is relatively short around approximately 1,500 bp. Second, ten regions in the 16S rDNA gene sequence are common among most bacteria (conserved region) and are separated into nine diverse regions (hypervariable regions). Third, the gene sequences registered in public databases are increasing substantially, because the gene sequence is important information for identification and classification in bacterial taxonomic studies. (40). The scheme of the ribosome complex and 16S rDNA gene is shown in Figure 3

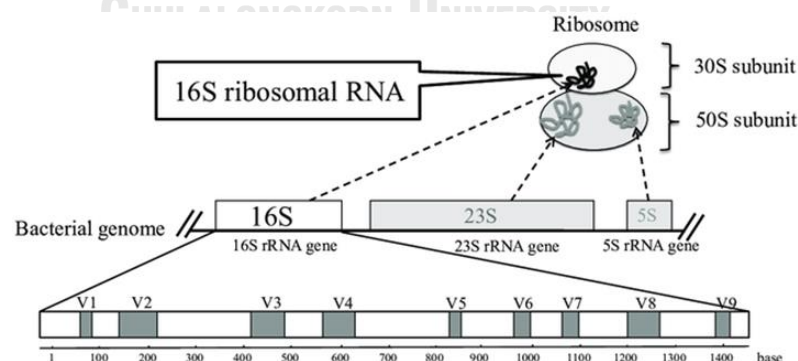


Figure 3: The schematic of ribosome complex and 16S rDNA gene

The white and grey boxes indicate conserved regions and hypervariable regions (V1-V9) respectively. The bold arrows are shown the approximate positions of universal primers on the 16S rDNA gene sequence of *Escherichia coli* (40).

5. 18S ribosomal DNA gene and Internal transcribed space region

18S ribosomal DNA or 18S rDNA is the essential component of the eukaryotic cells in a small ribosomal eukaryotic subunit (the 40S) which is the homolog of 16S rDNA in prokaryotes and mitochondria, thus one is widely used in phylogenetic analysis and environmental biodiversity screening for eukaryotes (42).

The internal transcribed spacer (ITS) includes two spacers, ITS1 and ITS2, separated by the 5.8S rDNA gene, and has a high degree of sequence variation with approximately 650 bp as shown in Figure 4. These spacer regions evolve much faster than other coding regions since the occurrence of substitutes in these spacers might be considered neutral mutations without any restriction (43). The 5.8S rDNA gene shows a weakened rate of evolutionary change whereas the spacers are a higher level of sequence variation which be used to aggregate phylogenetic relationships and even higher taxonomic levels. (44). There is a large amount of research available concerning the usefulness of ITS sequences, consequently, ITS sequences as excellent markers for species distinction (43).

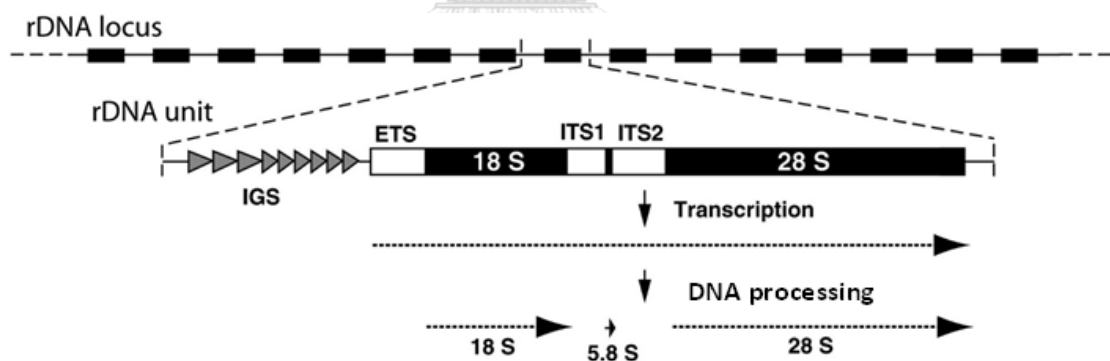


Figure 4: The schematic of the rDNA genes in eukaryotes

The positions of the three rDNA genes (18S, 5.8S, 28S) are indicated with solid boxes, while regions processed from the primary transcript are in open boxes (ETS, external transcribed spacer; ITS, internal transcribed spacer). The extent and direction of the transcribed region of each unit as well as the final mature rDNAs derived from that transcript are shown at the bottom as dotted arrows (45).

However, 18S rDNA is mainly used for high-resolution taxonomic studies of fungi, while the ITS1 and ITS2 are the most suitable fungal barcode markers and are widely used for analyzing fungal diversity in environmental samples due to their variable sequences, conserved primers and multicopy nature (46). Therefore, ITS is more variable and thereby, more suitable as the genetic marker to measure intraspecific genetic diversity (42, 47).

6. Third-generation sequencing

Long-read technologies are the ones in third-generation sequencing that are overcoming all of the limitations in accuracy, throughput, and broadening the application domains at the genome which offers several advantages over short-read sequencing. (48). While short-read sequencers such as Illumina's NovaSeq, HiSeq, NextSeq, and MiSeq instruments or Thermo Fisher's Ion Torrent sequencers produce reads of up to 600 bases, long-read sequencing technologies routinely generate reads over 10 kb (48, 49). All of these capabilities together with incessantly progressing accuracy, throughput, and cost reduction, have begun to make long-read sequencing an option for a broad range of applications in genomics for both model and non-model organisms. (50).

ONT with a portable MinION (512 nanopore flow cell channels), benchtop GridION (5 flow cells in a single module), and a high throughput PromethION (48 flow cells of 3000 nanopores each), was commercially released in 2014 (<https://nanoporetech.com/applications/dna-nanopore-sequencing> and <https://nanoporetech.com/how-it-works>), and since then have become suitable for an increasing number of applications (48, 51). These sequencers measure the ionic current fluctuations when single-stranded nucleic acids pass through biological nanopores (52). Long double-stranded DNA molecules are first bound with a processive enzyme. The DNA molecule translocates through a protein nanopore as shown in Figure 5. When the complex encounters a nanopore, one of the DNA strands enters and translocates through the pore, and the translocation rate is regulated by DNA polymerase synthesis. The processive enzyme enables the DNA to be continuously and processive "ratched" through it. As a DNA strand passes through

the pore, it interferes with a current being applied to the nanopore. Each nucleotide provides a unique characteristic electronic signal which is recorded as a current interruption event. The recording is in real-time and while 10kb reads are a reasonable output which refers to the theory 100s of kb of DNA can pass through each nanopore and be detected. Once DNA has left a nanopore, the pore is available for use by a different DNA molecule (51). The scheme of the nanopore sequencing system is shown in Figure 6.

Because of its small, handheld size, the MinION has the potential for many applications where portability and or space requirements are at a premium. An overview of the nanopore sequencing process is shown in Figure 7. Although the error rate is relatively high as with other high throughput sequencing methods, this can be circumvented by the large number of molecules that can be sequenced. Furthermore, an improved flow cell R10.4.1 revision of the R10.4 pore is currently available with a new motor E8.2. helps to reduce errors. It will offer the high accuracy of the Q20+ (> 99% accuracy) chemistry, enable duplex sequencing and base modification calling (<https://nanoporetech.com/about-us/news/oxford-nanopore-technology-updates-show-consolidations-and-updates-single-high>). The new motor inherently enables somewhat faster speeds and several favorable properties for high-accuracy base-calling with tighter speed distribution, better-resolved signal levels, and fewer missteps. To support both high accuracy and high-yield use cases, instrument software will enable controlling the flow cell temperature - perhaps even during a run as summarized in Figure 8.

Nanopore technology has been used to sequence environmental and metagenomic samples has been used for bacterial strain identification. Viral genomes, environmental surveillance, and haplotyping have been performed using the MinION. It is also able to identify base modifications and also offers direct DNA sequencing, as well as PCR-free cDNA sequencing. Thus, nanopore sequencing has the potential to offer relatively low-cost DNA sequencing, environmental monitoring, and genotyping (51, 53).

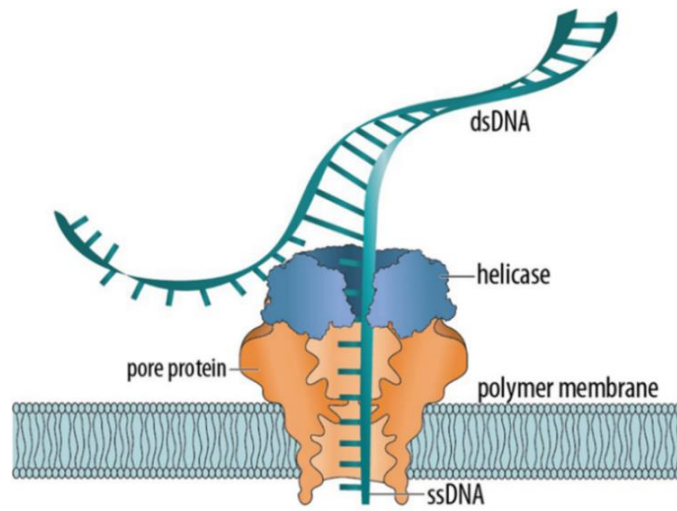


Figure 5: The schema of a DNA molecule translocating a protein nanopore

The double-stranded DNA (dsDNA) is split by a helicase enzyme, allowing only a single strand (ssDNA) to pass while slowing it enough to achieve sufficient resolution for sequencing (54).

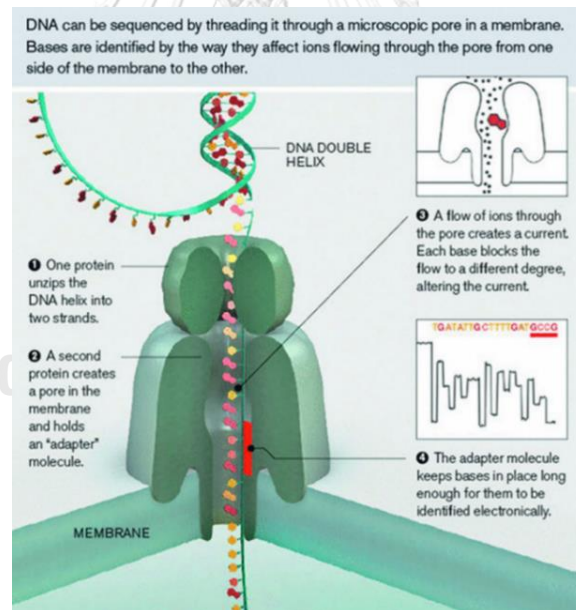


Figure 6: The schema of the nanopore sequencing system

(1) The upper protein is used to make the DNA molecule single-stranded. (2) The second protein forms a nanopore in a membrane. It also contains an adaptor molecule. (3) Each base obstructs the flow to a different degree. (4) The adaptor is used to reduce the speed of passing DNA through the pore, which is necessary for the exact identification of the DNA strand base composition (55).

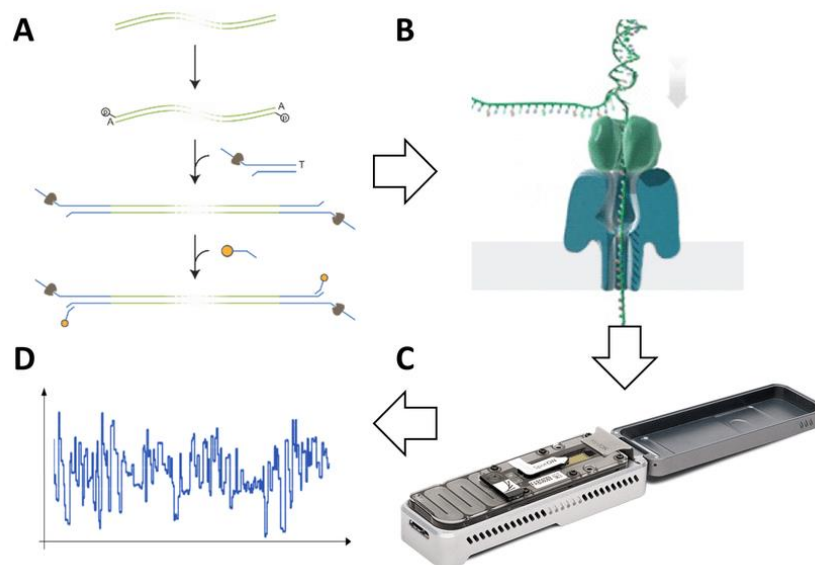


Figure 7: The Overview of the nanopore sequencing process using MinION

DNA is prepared (A) and fed to a nanopore (B), which is embedded in the MinION Flow Cell membrane (C). The MinION sequences and produces ionic signals (D) that can be analyzed to estimate DNA sequences (56).

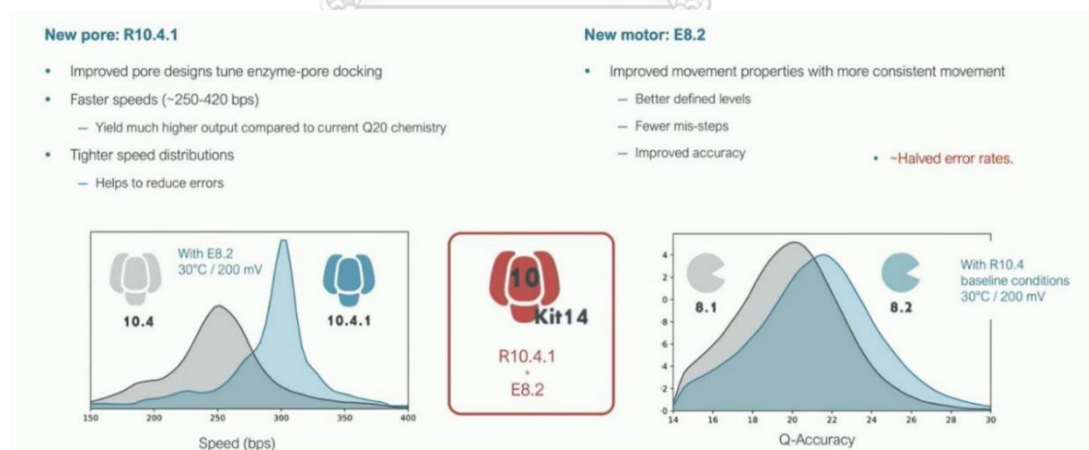


Figure 8: The summary of new chemistry, kit 14

Which will soon be available and which combines an R10.4.1 revision of the R10.4 pore currently available with a new motor E8.2.

CHAPTER III

METHODOLOGY

1. Research workflow

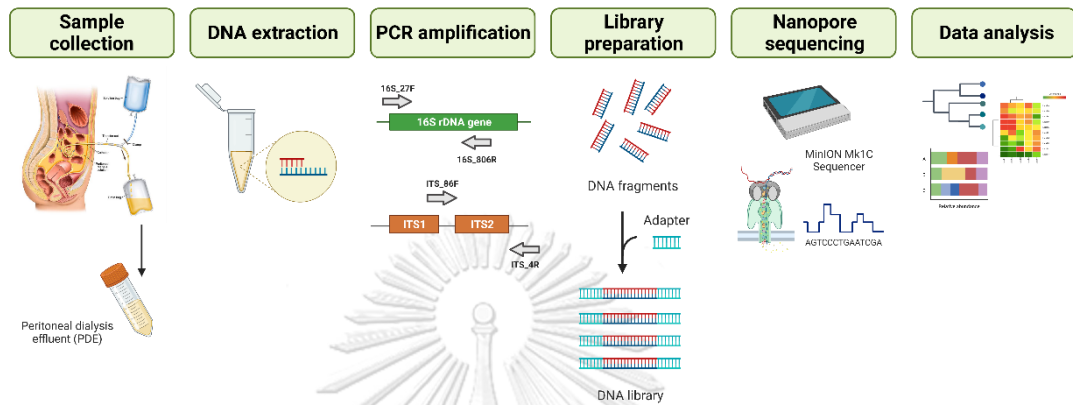


Figure 9: Research workflow of metagenomic analysis based on amplicon sequencing from PDE samples

This study workflow consists of the major steps of sample collection, DNA extraction, PCR amplification, Library preparation, Nanopore sequencing and finally, data analysis.

2. Sample size calculation

The following simple formula can be used:

$$n = \frac{Z^2 p(1 - p)}{d^2}$$

where n = sample size,

Z = Z statistic for a level of confidence,

p = expected proportion,

d = precision

Z statistic (Z): For the level of confidence of 90%, which is conventional, the Z value is 1.65. This study presents the results with 90% confidence intervals (CI).

Expected proportion (p): This is the proportion (prevalence) estimated by the study. In this study, the prevalence in a sample from the previous study (57) is 31%. So, $p = 0.31$.

Precision (d): It is very important to understand this value well. From the formula, it can be conceived that the sample size varies inversely with the square of precision (d²). In this study, the precision for this estimate is 10%. So, $d = 0.10$.

When substituting in the formula, the sample size will be:

$$n = \frac{1.65^2 \times 0.31 \times (1 - 0.31)}{0.10^2}$$

$$n = 58.234$$

Therefore, the estimated sample size of this study will be at least 59.

3. Participants

In this study, 104 peritoneal dialysis effluent (PDE) samples were obtained from patients at the peritoneal center of 22 hospitals in Thailand between 2020 and 2022. The samples were leftover from the Thailand-Peritoneal Dialysis Outcomes and Practice Patterns Study (Thailand-PDOPPS) to follow up on ESKD patients undergoing PD in Thailand which was approved by the Institutional Review Board of the Faculty of Medicine, Chulalongkorn University (COA No. 1544/2020, IRB No. 499/58). Furthermore, the Institutional Review Board of the Faculty of Medicine, Chulalongkorn University, approved the protocol of this study (COA No. 0754/2022, IRB No. 0253/65).

All participants are over 18 years old and have ESKD undergoing continuous ambulatory peritoneal dialysis (CAPD) and automated peritoneal dialysis (APD) for more than 1 month. The patients had to satisfy the following 2 in 3 inclusion criteria: (1) PDE from the first episode of infection that was observed cloudy; (2) Peritonitis caused by the infection has been reported; (3) A white blood cell count more than 100 cells and/or the percentage of polymorphonuclear neutrophils (PMNs) more than 50%. The patients under 18 years who underwent hemodialysis (HD), acute peritoneal dialysis, or combination renal replacement therapy were excluded from this study.

4. Sample processing and DNA extraction

The sample processing and DNA extraction were processed by the Center of Excellence in Kidney Metabolic Disorders, Chulalongkorn University, Bangkok, Thailand. Briefly, the samples were collected at 50 mL and centrifuged for 15 min in a microcentrifuge at 12,000 rpm followed by discarding the supernatant. The pellet was suspended in 400 μ L of sorbitol buffer with 50 U of Lyticase enzyme (Sigma-Aldrich Pte. Ltd., Singapore), incubated at 30°C for 60 min to break the cell, and centrifuged at 12,000 rpm for 5 min followed by discarding the supernatant. Then, 567 μ L of 1M TE buffer, 3 μ L of 10% SDS (Sigma-Aldrich, Singapore), 10 μ g/mL of Lysozyme enzyme (Merck, Germany), and 5 μ g of mg/ml of Proteinase K (Worthington-Biochem, USA) were added and incubated at 65°C for 90 min to break the proteins and inhibit RNases. Finally, the samples were centrifuged for 5 min in a microcentrifuge at 12,000 rpm and the pellets were collected and resuspended with 200 μ L sterile water. The total genomic DNA (gDNA) was extracted using the magLEAD 12gC system (Precision System Science, Japan), following the manufacturer's protocol. DNA quantity and quality were evaluated using spectrophotometry and agarose gel electrophoresis. The DNA was stored at -20 °C until use.

5. 16S rDNA gene amplification

The amplification of the 16S rDNA gene based on three primer pairs was summarized in Table 3. The primer pair 1 (16S_27F/16S_1492R) provided the amplification and sequencing of the full-length 16S rDNA gene (1500 bp) for the classification of bacterial species. The primer pair 2 (16S_341F/16S_806R) was commonly used for V3-V4 region (500 bp) amplification and the taxonomic classification of bacteria based on short-reads Illumina platform. We validated the primer pair 3 (16S_27F/16S_806R) for amplification of the V1-V4 region (800 bp) to classify bacterial community at the species level.

The PCR products were amplified using Phusion™ Plus DNA Polymerase (Thermo Fisher Scientific, USA) to avoid errors during amplification. The PCR reaction was conducted in a total volume of 20 μ L containing inner primer pairs (0.25 μ M each) and the barcoded outer primer mixture from PCR Barcoding

Expansion 1-96 kit (EXP-PBC096; Oxford Nanopore Technologies, UK). The PCR components and temperature cycling conditions were summarized in Table 4 and Table 5, respectively. The PCR products were examined with 1% agarose gel electrophoresis and purified using QIAquick Gel Extraction Kit (Qiagen, Germany), following the manufacturer's protocol.



Table 3: Primers used for 16S rDNA and ITS amplifications

Targeted gene	Primer pair	Primer	Sequence (5' → 3')	Variable region	Approximately Product size (bp)
16S rDNA	1	16S_27F	<u>TTTCTGTTGGTGCTGATATTGCAGAGTTTGATCMTGGCTCAG</u>	V1-V9	1500
		16S_1429R	<u>ACTTGCCCTGTCGCTCTATCTTCGGACTACHVGGGTWTCTAAT</u>		
	2	16S_341F	<u>TTTCTGTTGGTGCTGATATTGCCCTACGGGNGGCWGCAG</u>	V3-V4	500
		16S_806R	<u>ACTTGCCCTGTCGCTCTATCTTCGGACTACHVGGGTWTCTAAT</u>		
	3	16S_27F	<u>TTTCTGTTGGTGCTGATATTGCAGAGTTTGATCMTGGCTCAG</u>	V1-V4	800
		16S_806R	<u>ACTTGCCCTGTCGCTCTATCTTCGGACTACHVGGGTWTCTAAT</u>		
ITS	4	ITS_1F	<u>TTTCTGTTGGTGCTGATATTGCTCCGTAGGTGAACCTGCGG</u>	ITS1-ITS2	700
		ITS_4R	<u>ACTTGCCCTGTCGCTCTATCTTCTCCTCCGCTTATTGATATGC</u>		
	5	ITS_1F	<u>TTTCTGTTGGTGCTGATATTGCTCCGTAGGTGAACCTGCGG</u>	ITS1	300
		ITS_2R	<u>ACTTGCCCTGTCGCTCTATCTTCGCTGCGTTCTTCATCGATGC</u>		
	6	ITS_86F	<u>TTTCTGTTGGTGCTGATATTGCGTGAATCATCGAATCTTTGAA</u>	ITS2	400
		ITS_4R	<u>ACTTGCCCTGTCGCTCTATCTTCTCCTCCGCTTATTGATATGC</u>		

Underlined sequences are specific regions for the 16S rDNA gene and ITS.

Table 4: PCR reaction components for 16S rDNA amplification

Components	PCR1 Volume (μ L)	PCR2 Volume (μ L)
5X Phusion™ Plus buffer	4	4
10 mM dNTPs	0.4	0.4
10 μ M Forward primer/barcode	0.5	0.25
10 μ M Reverse primer/barcode	0.5	0.25
Phusion™ Plus DNA polymerase	0.2	0.2
Nuclease-free water	13.4	13.9
Template DNA	1	1
Total Volume	20	20

Table 5: Thermal cycling for 16S rDNA amplification

PCR cycling step	Temperature	Time	Cycle
Initial denaturation	98°C	30 sec	1
Denaturation	98°C	10 sec	
Annealing	60°C	10 sec	25
Initial extension	72°C	50 sec	
Final extension	72°C	5 min	1

6. ITS region amplification

The fungal ITS region was amplified using three primer pairs as also shown in Table 3. The primer pair 4 (ITS_1F/ITS_4R) provided the amplification and sequencing of the full-length ITS region, including 5.8S (700 bp), for the classification of fungal species. The primer pair 5 (ITS_1F/ITS_2R) was the partial ITS1 region (300 bp), while the primer pair 6 (ITS_86F/ITS_4R) was commonly used for the partial ITS2 region (400 bp) with a longer targeted length.

To avoid error base incorporation, DNA was amplified by Ultra HiFi DNA Polymerase (TIANGEN Biotech, China). The total 20 μ L PCR reaction consisted of inner primer pairs (0.25 μ M each) and the barcoded outer primer mixture from PCR Barcoding Expansion 1-96 kit (EXP-PBC096; Oxford Nanopore Technologies, UK).

The PCR reaction mixtures and thermal profile were revealed in Table 6 and Table 7, respectively. The 1% agarose gel electrophoresis was applied for the PCR product size visualization. The barcoded libraries were purified by QIAquick Gel Extraction Kit (Qiagen, Germany), following the manufacturer's protocol.

Table 6: PCR reaction components for ITS amplification

Components	PCR1 and PCR2 Volume (μL)
2X Ultra HiFi DNA polymerase	10
PCR Enhancer	4
10 μM Forward primer/barcode	0.5
10 μM Reverse primer/barcode	0.5
Nuclease-free water	3
Template DNA	2
Total Volume	20

Table 7: Thermal cycling for ITS amplification

PCR cycling step	Temperature	Time	Cycle
Initial denaturation	94°C	2 min	1
Denaturation	98°C	10 sec	35 for PCR1 / 15 for PCR2
Annealing	60°C	10 sec	
Initial extension	68°C	45 sec	
Final extension	68°C	1 min	1

7. Nanopore library preparation

The purified libraries were quantified using Quant-iT™ dsDNA High Sensitivity Assay Kits for the Qubit™ 4 Fluorometer (Thermo Fisher Scientific, US) and then equimolarly pooled for multiplexing. The pooled library was purified using 0.5X (for 16S rDNA gene) and 0.8X (for ITS2) Agencourt AMPure XP beads (Beckman Coulter, USA). Then, the library was subjected to end repair and adaptor ligation steps using Ligation Sequencing Kit (SQK-LSK112 and SQK-LSK114 for 16S rDNA gene and ITS2, respectively). Finally, the pooled DNA library was sequenced via the

MinION™ Mk1C (Oxford Nanopore Technologies, UK) using R10.4 flow cell (FLO-MIN112) for 16S rDNA gene and R10.4.1 flow cell (FLO-MIN114) for ITS2.

8. Data analysis workflow

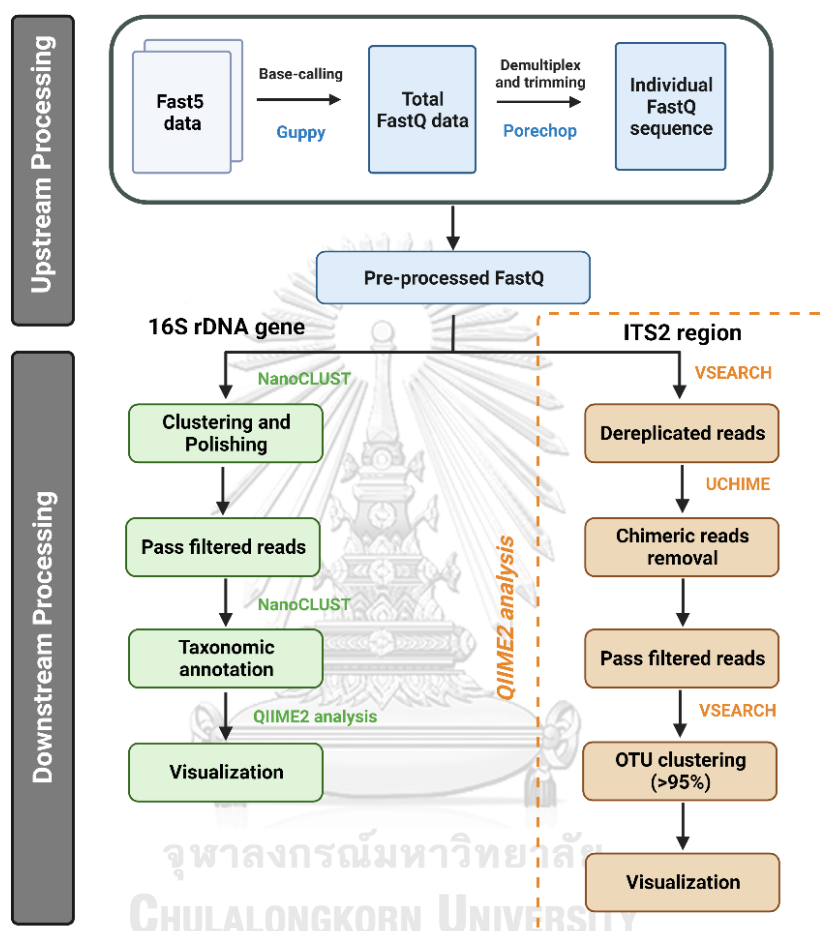


Figure 10: Data analysis workflow of metagenomic analysis based on amplicon sequencing from PDE samples

This data analysis pipeline was applied for bacterial and fungal classification using nanopore sequencing data of the 16S rDNA gene and ITS2 region, respectively.

9. Base-calling and data processing

The FAST5 data were base called by Guppy basecaller version 6.0.7 (Oxford Nanopore Technologies, UK) with a super-accuracy model to generate pass reads in FASTQ format with a minimum acceptable quality score at $Q>10$ (58). Then, the quality of reads was examined by MinIONQC (59). The FASTQ sequences were demultiplexed and adaptor-trimmed by using Porechop version 0.2.4 (<https://github.com/rrwick/Porechop>).

10. Bacterial classification based on 16S rDNA gene sequencing

The filtered reads were clustered, polished, and taxonomically classified by NanoCLUST (60) based on the V1-V4 region of 16S rDNA gene sequences from the Ribosomal Database Project (RDP) database (61). The relative abundance and taxonomic assignment data were converted to the QIIME2 data format to demonstrate the richness and evenness of bacterial species based on their taxa abundances using a plug-in implemented for QIIME2 software v2021.2 (62). The normalized data were visualized by Rstudio version 4.2.2.

11. Fungal classification based on ITS sequencing

The FASTQ data were continually processed by the QIIME2 analysis pipeline v2021.2 (62). The chimeric reads were removed by the UCHIME algorithm (63). The filtered reads were clustered into Operational taxonomic units (OUT) at 95% similarity by VSEARCH (64). Then, these passed filtered sequences were classified by the VSEARCH algorithm based on the SILVA database (<https://www.arb-silva.de/>). The alpha diversity (Chao1 and Shannon indexes) was estimated based on their taxa abundances. The relative composition of fungal taxonomy was carried out by GraphPad Prism 9.5.0.

CHAPTER IV

RESULTS

1. Selection of primers for bacterial 16S rDNA gene amplification

The V1-V9, V3-V4, and V1-V4 variable regions were amplified by three-primer pairs from five representative PDF samples (S01-S05) and compared the PCR product results with 1% agarose gel electrophoresis (Figure 11). The primer pair 1 yielded the positive band of the full-length 16S rDNA in 3/5 samples (60%). However, the high-density band was obtained in only 1 sample whereas the faint bands were in the other 2 samples. In contrast, 5/5 samples (100%) amplified products were obtained from the primer pair 2. Nevertheless, the non-specific amplicons (400, 450 and 900 bp) were observed in some samples. Interestingly, primer pair 3 provided a sharp and high-density band in 5/5 samples (100%) without non-specific PCR products. Therefore, this primer pair was selected for further validation and analysis.

Figure 12 showed the representative result of 16S rDNA amplification using 16S_27F and 16S_806R primers. Among 104 PDE samples, 15 samples were unable to amplify whereas 89 samples yielded a positive band as expected. However, non-specific PCR products can be observed in some samples. Therefore, the targeted amplicons were cut and purified by QIAquick Gel Extraction Kit (Qiagen, Germany).

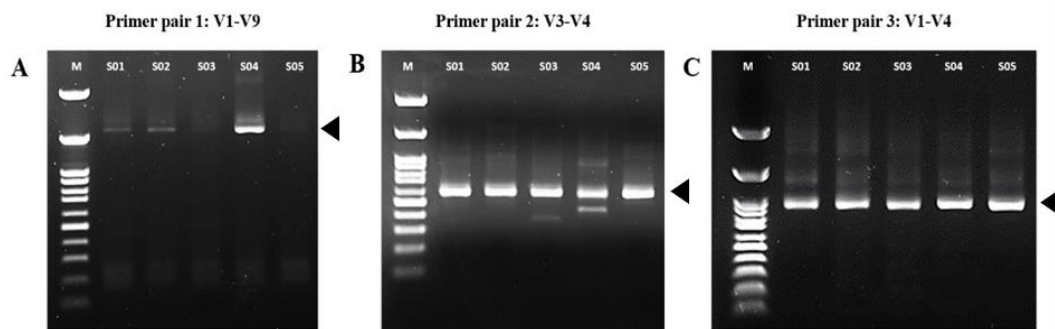


Figure 11: The 1% agarose gel electrophoresis for comparisons among 3 primer pairs specific to bacterial 16S rDNA PCR products

(A) The V1-V9 amplified products (~1,500 bp) from primer pair 1 (16S_27F/16S_1492R). (B) The V3-V4 PCR products (~500 bp) using primer pair 2 (16S_341F/16S_806R). (C) The V1-V4 amplicons (~800 bp) are based on the primer pair 3 (16S_27F/16S_806R). M: 100 bp ladder marker. S01-S05: representative PDF samples. The triangle indicated the expected band.

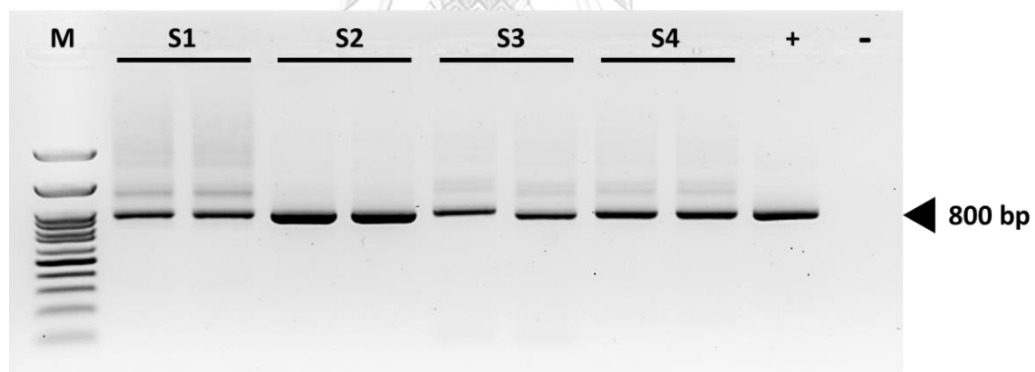


Figure 12: The representative PCR products obtained from the amplification of the 16S rDNA gene using 16S_27F/16S_806R primers

M: 100 bp ladder marker. S1-S4: representative PDE samples. + and – are positive and negative controls, respectively. The triangle indicated the expected band (approximately 800 bp).

2. Diversity of bacterial in peritoneal dialysis effluent

The bacterial 16S rDNA (V1-V4 variable region) was sequenced with a high-throughput MinION™ platform (Oxford Nanopore Technologies, UK). In this study, 1,341,989 total raw reads were obtained with 15,079 average reads per sample. The average classified reads were 10,656 reads per sample as summarized in Table 8. The rarefaction analysis was applied to estimate whether there was sufficient sequence coverage to reliably classify all samples. The result showed sufficient sequencing depth for diversity in 89 PDE samples (Figure 13). Alpha diversity (richness and evenness analysis) was summarized in Table 9.

Table 8: Summary of 16S rDNA sequencing data

Targeted gene	Total raw reads	Average reads/Sample	Average classified reads/Sample
16S rDNA	1,341,989	15,079 ± 11,214	10,656 ± 7,762

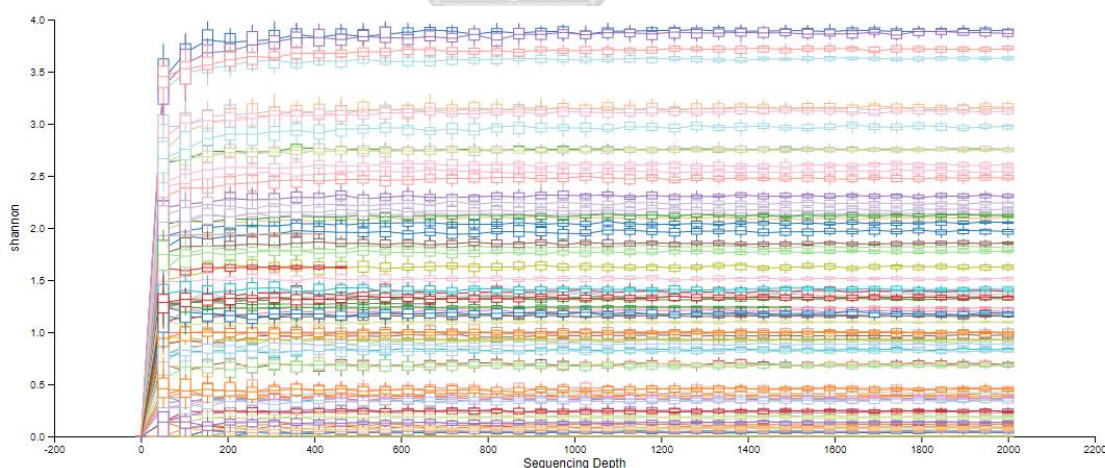


Figure 13: Rarefaction curve analysis of 16S rDNA gene

X-axis represented the sequencing depth and Y-axis represented the Shannon diversity index. Each color line represented different samples.

Table 9: Alpha diversity indexes (Chao1 and Shannon) of bacteria

Targeted gene	Chao1 index	Shannon index
16S rDNA	8.15 ± 8.06	1.24 ± 1.05

3. The relative abundance of bacterial classification

The relative abundance of bacterial composition in 89 PDE samples was classified. At the phylum level, the dominant bacteria were Firmicutes, Proteobacteria and Actinobacteria (Figure 14). The relative abundance of bacteria at the genus level was demonstrated in Figure 15. Five major bacterial genera were *Escherichia/Shigella*, *Streptococcus*, *Staphylococcus*, *Phyllobacterium* and *Lactococcus*. Several abundant bacterial species were identified in PD patients (Figure 16). The result showed that *Escherichia coli* was the most bacterial species followed by *Phyllobacterium myrsinacearum*, *Streptococcus gallolyticus*, *Staphylococcus epidermidis*, and *Shewanella algae*, respectively.

The heatmap visualized the hierarchical clustering of bacterial diversity and showed the top 35 abundances of bacteria at the species level. All subjects were divided into 8 clusters according to the microbial community patterns in the samples (Figure 17). The dominant bacterial community included *Candidatus Rhizobium* (Cluster 1), *Lactococcus garvieae* (Cluster 2), *Phyllobacterium myrsinacearum* (Cluster 3), *Streptococcus gallolyticus* (Cluster 4) and *Staphylococcus epidermis* (Cluster 6). The *Escherichia coli* dominated in Clusters 7 and Clusters 8 which were distinguished by the relative abundance greater than 70% and less than 70%, respectively. However, other microbial community patterns were classified in Cluster 5.

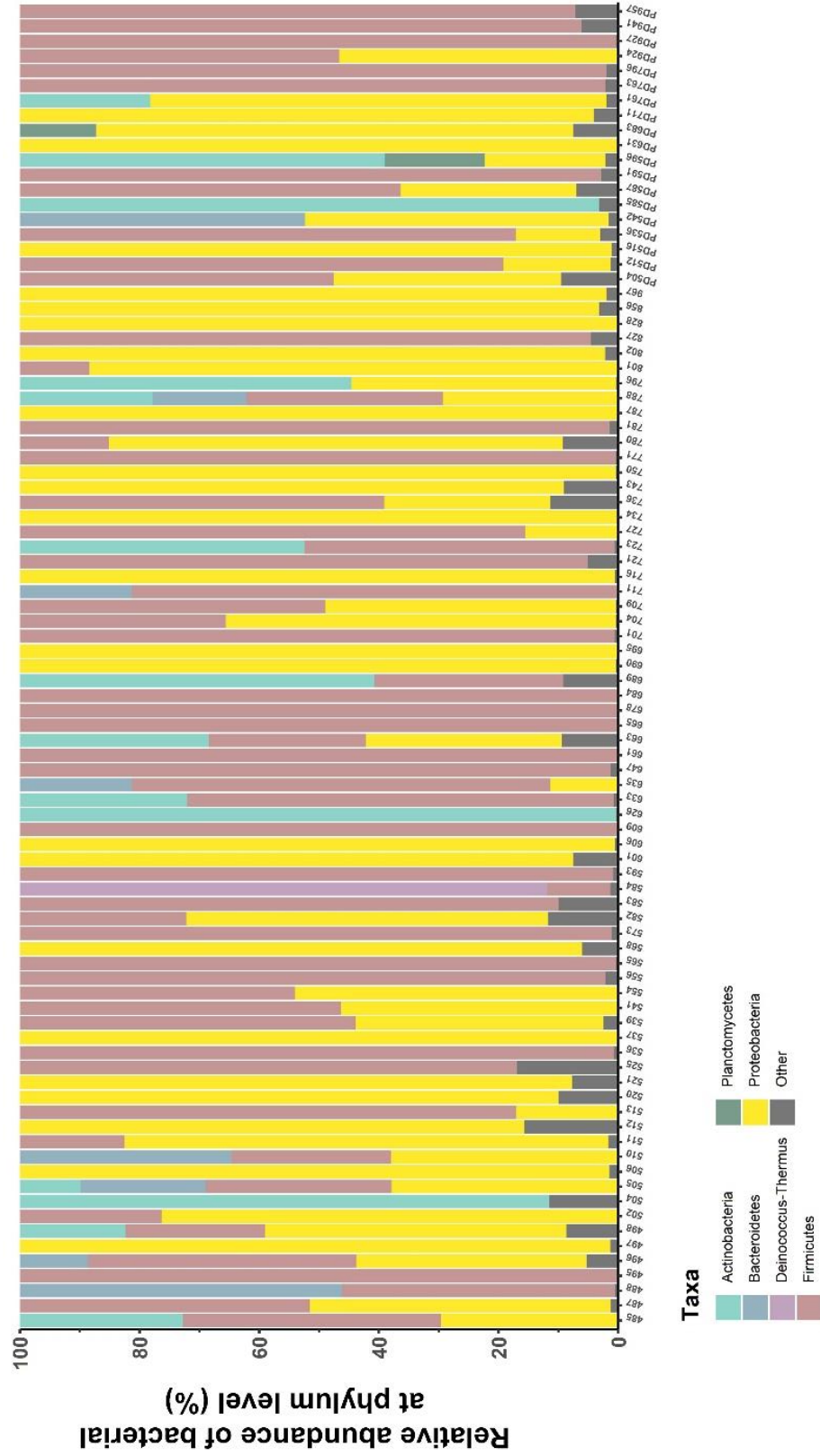


Figure 14: The taxonomic composition of bacterial classification in 89 PDE samples

The relative abundance (%) of 6 bacteria at the phylum level. The colored bar charts represent the different bacterial phyla. The bacterial taxonomy of less than 10% was classified as other.

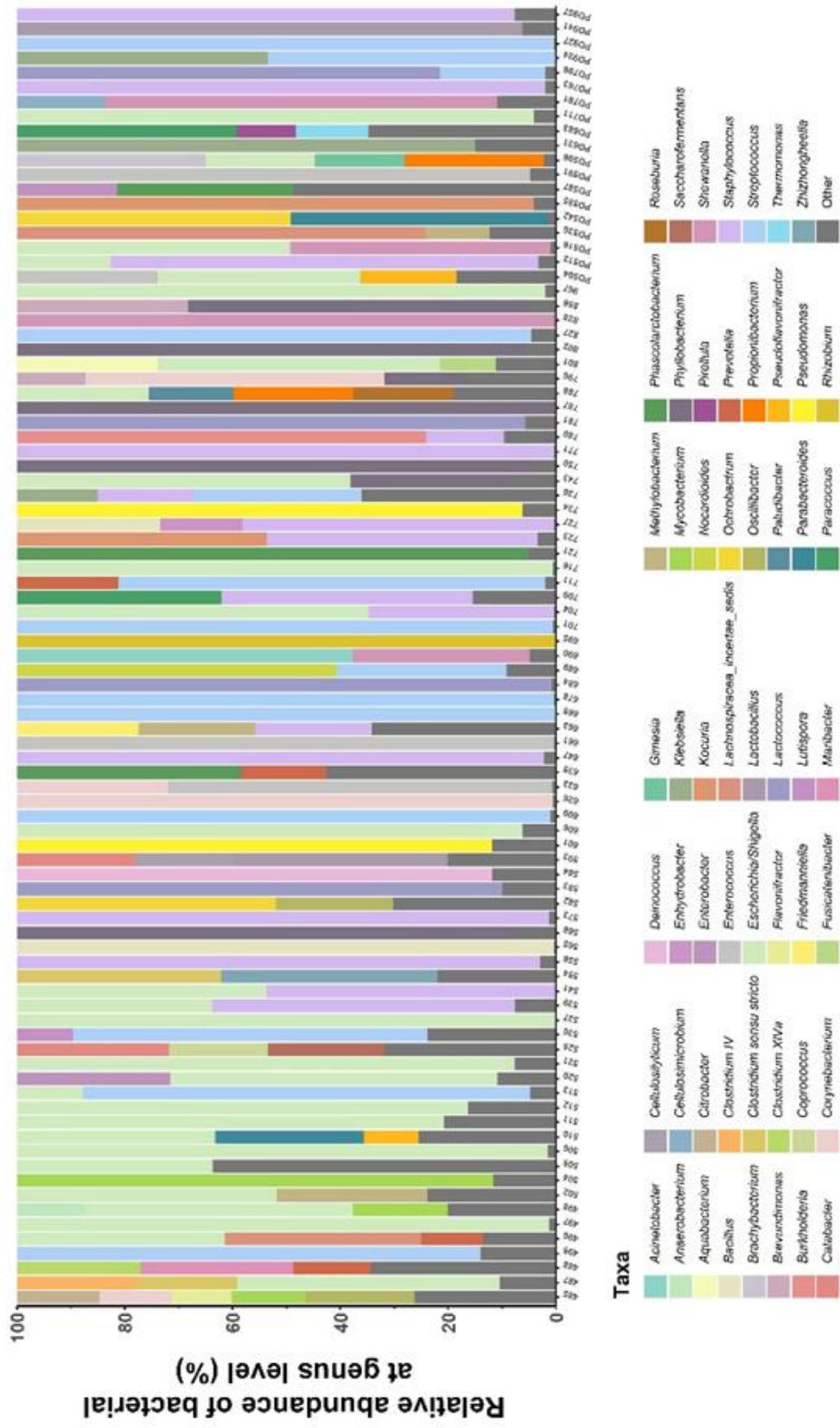


Figure 15: The relative abundance (%) of 55 bacteria at the genus level

The colored bar charts represent the different bacterial genera. The bacterial taxonomy of less than 10% was classified as other.

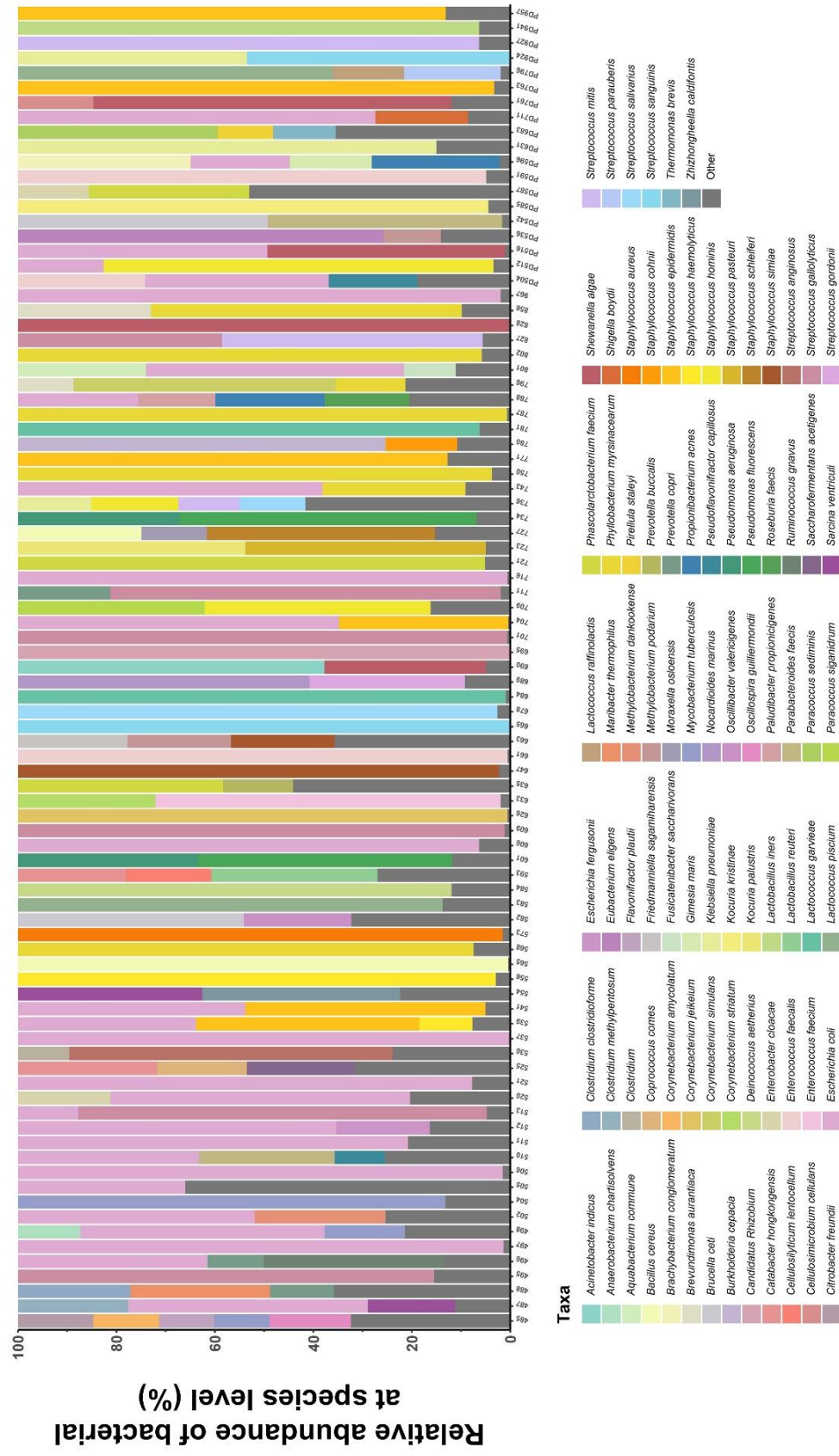


Figure 16: The relative abundance (%) of 84 bacteria at the species level

The colored bar charts represent the different bacterial species. The bacterial taxonomy of less than 10% was classified as other.

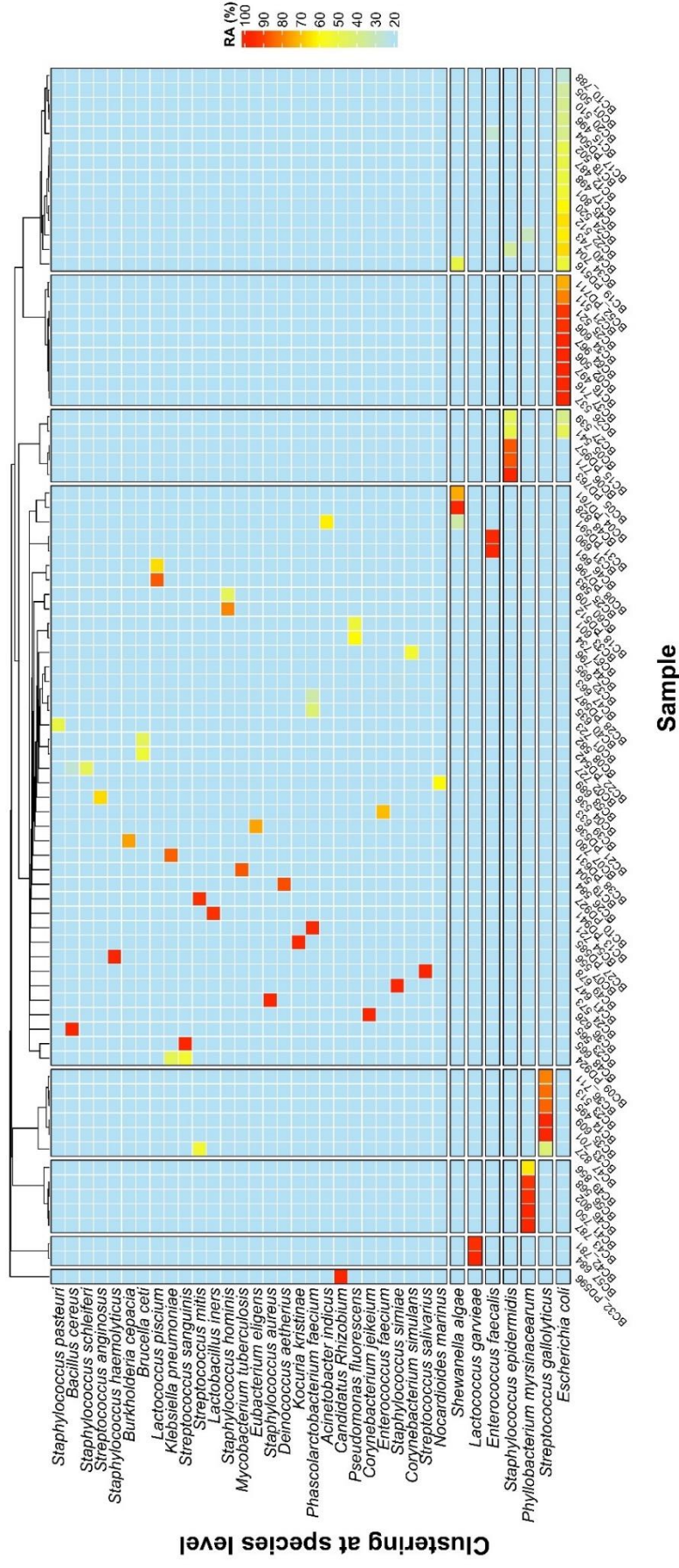


Figure 17: Heatmap visualized the hierarchical clustering of the bacterial community of each sample based on the analysis of the 35 most abundant species

The color represented the relative abundance (RA) of percentage (%) for bacterial species.

4. Bacterial identification between metagenomic and traditional culture methods

Among the 89 PDE samples, bacterial species were identified from only 56 samples (62.92%) based on the traditional culture method whereas all samples (100%) can be classified through metagenomic approaches (Figure 18). Comparison between metagenomic and traditional culture methods for bacterial classification in 56 samples, concordant results from both techniques were observed in 42/56 samples (75%). Briefly, the dominant bacterial species were *E. coli* (8 cases), *S. epidermidis* (6 cases), *K. pneumoniae* (3 cases), *S. aureus* (3 cases), *E. faecalis* (2 cases), *P. aeruginosa* (2 cases), *S. mitis* (2 cases) and 16 other bacterial species (1 case each) as summarized in Table 10. On the other hand, 14/56 samples (25%) demonstrated different results between metagenomics approaches and traditional culture methods as shown in Table 11. Interestingly, the metagenomic approaches can be applied for bacterial classification in 33/89 samples (37.08%) which are negative for the traditional culture method. The metagenomic result was summarized in Table 12.

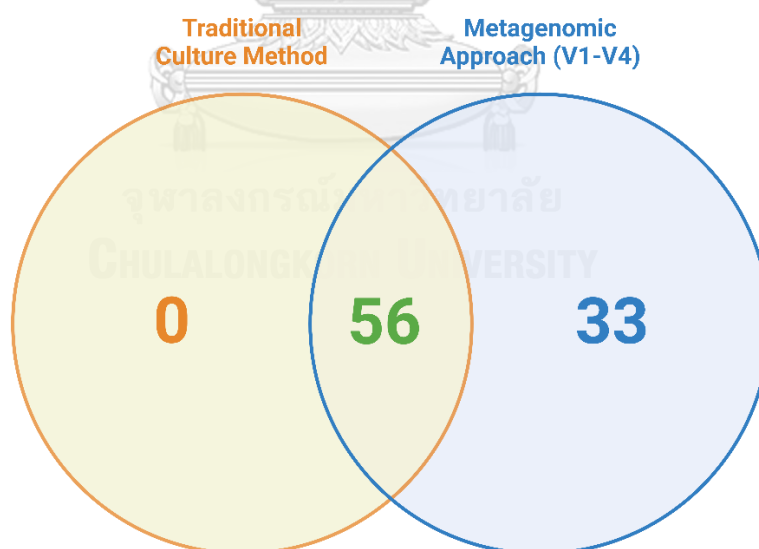


Figure 18: Venn diagram illustrated the number of PDE samples that can be classified for bacterial species based on the metagenomic approach (V1-V4) and traditional culture method

The numbers in the overlapping circles showed positive results in both methods.

Table 10: Summary of concordant bacterial species in both methods

Bacterial Species	Samples ID	Number of cases (%)
<i>A. indicus</i>	PD591	1/42 (2.38%)
<i>B. cepacia</i>	780	1/42 (2.38%)
<i>C. Rhizobium</i>	PD596	1/42 (2.38%)
<i>C. freundii</i>	485	1/42 (2.38%)
<i>C. simulans</i>	796	1/42 (2.38%)
<i>C. striatum</i>	568	1/42 (2.38%)
<i>C. striatum</i>	633	1/42 (2.38%)
<i>E. faecium</i>		
<i>E. coli</i>	505, 487, 497, 510, 511, 716, 750, PD711	8/42 (19.05%)
<i>E. cloacae</i>	520	1/42 (2.38%)
<i>E. faecalis</i>	690, 661	2/42 (4.76%)
<i>K. pneumoniae</i>	736, PD924, PD631	3/42 (7.15%)
<i>L. garvieae</i>	684	1/42 (2.38%)
<i>P. aeruginosa</i>	734, 601	2/42 (4.76%)
<i>S. algae</i>	828	1/42 (2.38%)
<i>S. aureus</i>	573, 647, 663	3/42 (7.15%)
<i>S. epidermidis</i>	541, 539, 711, 771, PD763, PD957	6/42 (14.29%)
<i>S. haemolyticus</i>	556	1/42 (2.38%)
<i>S. hominis</i>	709	1/42 (2.38%)
<i>S. pasteurii</i>	723	1/42 (2.38%)
<i>S. schleiferi</i>	727	1/42 (2.38%)
<i>S. anginosus</i>	536	1/42 (2.38%)
<i>S. gallolyticus</i>	495	1/42 (2.38%)
<i>S. mitis</i>	827, PD927	2/42 (4.76%)

Table 11: Summary of different bacterial species between the metagenomic approach and traditional culture method

Sample ID	Traditional culture method result	Top 3 of metagenomic approach result (%abundance)
496	<i>K. kristinae</i>	<i>E. coli</i> (38.54%), <i>R. gnavus</i> (36.54%), <i>P. copri</i> (11.45%)
502	<i>O. anthropi</i>	<i>E. coli</i> (48.22%), <i>M. dankookense</i> (26.55%), <i>C. saccharolyticum</i> (7.73%)
506	<i>P. aeruginosa</i>	<i>E. coli</i> (98.70%), <i>B. pullicaecorum</i> (0.68%), <i>S. paludicola</i> (0.63%)
525	<i>S. aureus</i>	<i>C. hongkongensis</i> (28.33%), <i>S. acetigenes</i> (21.85%), <i>C. comes</i> (18.24%)
554	<i>Corynebacterium</i> sp.	<i>Z. caldiformis</i> (40.20%), <i>S. ventriculi</i> (37.47%), <i>A. ruhlandii</i> (5.99%)
582	<i>P. aeruginosa</i>	<i>B. ceti</i> (48.96%), <i>O. valericigenes</i> (21.84%), <i>A. xylosoxidans</i> (7.65%)
593	<i>R. radiobacter</i>	<i>L. reuteri</i> (33.81%), <i>C. hongkongensis</i> (21.98%), <i>C. lentocellum</i> (17.36%)
665	<i>S. epidermidis</i>	<i>S. sanguinis</i> (100%)
695	<i>M. tuberculosis</i>	<i>B. conglomeratum</i> (35.84%), <i>P. acnes</i> (26.55%), <i>E. coli</i> (20.58%)
781	Coagulase Negative Staphylococcus (CONS)	<i>L. garvieae</i> (93.95%), <i>C. lentocellum</i> (2.21%), <i>E. coli</i> (1.24%)
788	<i>S. putrefaciens</i>	<i>E. coli</i> (24.51%), <i>P. acnes</i> (22.27%), <i>R. faecis</i> (17.22%)
PD512	<i>K. pneumoniae</i>	<i>S. hominis</i> (79.20%), <i>E. coli</i> (17.44%), <i>V. atypica</i> (0.71%)
PD542	<i>M. tuberculosis</i>	<i>B. ceti</i> (50.73%), <i>P. faecis</i> (47.73), <i>R. intestinalis</i> (1.48%)
PD941	<i>S. haemolyticus</i>	<i>L. iners</i> (93.77%), <i>P. staleyii</i> (4.15%), <i>M. podarium</i> (1.93%)

Table 12: Summary of bacterial species through the only metagenomic method

Sample ID	Top 3 of metagenomic approach result (%abundance)
488	<i>M. thermophilus</i> (28.32%), <i>C. clostridioforme</i> (22.94%), <i>P. copri</i> (12.99%)
498	<i>E. coli</i> (49.62%), <i>M. tuberculosis</i> (16.36%), <i>A. chartisolvans</i> (12.73%)
504	<i>M. tuberculosis</i> (86.92%), <i>C. segnis</i> (2.80%), <i>E. coli</i> (2.49%)
512	<i>E. coli</i> (64.79%), <i>E. fergusonii</i> (19.04%), <i>M. tuberculosis</i> (5.14%)
513	<i>S. gallolyticus</i> (83.13%), <i>E. coli</i> (12.31%), <i>B. ceti</i> (3.57%)
521	<i>E. coli</i> (92.49%), <i>F. magna</i> (7.51%)
537	<i>E. coli</i> (100%)
565	<i>B. cereus</i> (99.62%), <i>P. acnes</i> (0.30%), <i>B. weihenstephanensis</i> (0.08%)
583	<i>L. piscium</i> (86.47%), <i>D. aetherius</i> (9.74%), <i>L. raffinolactis</i> (3.79%)
584	<i>D. aetherius</i> (88.51%), <i>E. faecalis</i> (7.62%), <i>C. oryzae</i> (2.08%)
606	<i>E. coli</i> (93.77%), <i>M. podarium</i> (4.13%), <i>M. radiotolerans</i> (1.40%)
609	<i>S. gallolyticus</i> (98.93%), <i>L. piscium</i> (1.07%)
626	<i>C. jeikeium</i> (99.50%), <i>M. halophilus</i> (0.27%), <i>P. acnes</i> (0.23%)
635	<i>P. faecium</i> (41.69%), <i>P. buccalis</i> (14.21%), <i>O. valericigenes</i> (8.52%)
678	<i>S. salivarius</i> (97.45%), <i>S. warneri</i> (2.36%), <i>E. faecalis</i> (0.19%)
689	<i>N. marinus</i> (59.48%), <i>S. gordonii</i> (31.69%), <i>P. sediminis</i> (8.11%)
701	<i>S. gallolyticus</i> (99.54%), <i>E. coli</i> (0.46%)
704	<i>E. coli</i> (65.45%), <i>S. epidermidis</i> (34.55%)
721	<i>P. faecium</i> (94.92%), <i>B. luteolum</i> (3.95%), <i>P. stutzeri</i> (0.75%)
743	<i>E. coli</i> (62.44%), <i>P. myrsinacearum</i> (29.22%), <i>C. minuta</i> (8.34%)
787	<i>P. myrsinacearum</i> (99.53%), <i>O. pituitosum</i> (0.47%)
796	<i>L. piscium</i> (65.22%), <i>S. parauberis</i> (20.05%), <i>L. raffinolactis</i> (14.73%)
801	<i>E. coli</i> (52.48%), <i>A. commune</i> (26.08%), <i>F. saccharivorans</i> (10.55%)
802	<i>P. myrsinacearum</i> (94.42%), <i>B. vesicularis</i> (3.59%), <i>R. mucilaginis</i> (1.99%)
856	<i>P. myrsinacearum</i> (63.30%), <i>B. aurantiaca</i> (27.09%), <i>B. vesicularis</i> (4.72%)
967	<i>E. coli</i> (98.17%), <i>P. acnes</i> (1.83%)
PD504	<i>E. coli</i> (37.35%), <i>E. faecalis</i> (25.86%), <i>P. capillosus</i> (17.96%)
PD516	<i>E. coli</i> (51.20%), <i>S. algae</i> (48.80%)
PD536	<i>E. eligens</i> (74.34%), <i>M. podarium</i> (11.61%), <i>S. epidermidis</i> (7.05%)
PD585	<i>K. kristinae</i> (95.64%), <i>G. para-adiacens</i> (1.62%), <i>S. suis</i> (0.71%)
PD587	<i>P. faecium</i> (32.69%), <i>E. cloacae</i> (14.38%), <i>E. eligens</i> (8.00%)
PD683	<i>P. sediminis</i> (40.62%), <i>T. brevis</i> (12.76%), <i>P. staleyii</i> (11.20%)
PD761	<i>S. algae</i> (72.93%), <i>C. cellulans</i> (15.33%), <i>N. kribbensis</i> (5.45%)

5. Selection of primers for fungal ITS region amplification

The ITS1-ITS2, partial ITS1, and partial ITS2 regions of ten representative PDE samples (S01-S10) were amplified by three-primer pairs, and the PCR products were determined with 1% agarose gel electrophoresis (Figure 19). Primer pair 4 provided the positive band of the full-length ITS region (approximately 700 bp) in only 3/10 samples (30%), while primer pair 5 (approximately 300 bp) provided faint bands of the partial ITS1 in 10/10 samples (100%). However, the primer dimers (approximately 150 bp) were obviously observed in all samples using both primer pairs 4 and 5. Noticeably, primer pair 6 (approximately 400 bp) provided high-density bands in 9/10 samples (90%) without primer dimers. Nevertheless, non-specific PCR amplicons appeared in a few samples. Thus, the targeted bands were purified using QIAquick Gel Extraction Kit (Qiagen, Germany). Hence, primer pair 6 (ITS2_86F and ITS_4R) was selected for amplification of the partial ITS2 region in PDE samples (Figure 20). In total 104 PDE samples, the expected band was positive in 69 samples (66.35%) but negative in 35 samples (33.65%).

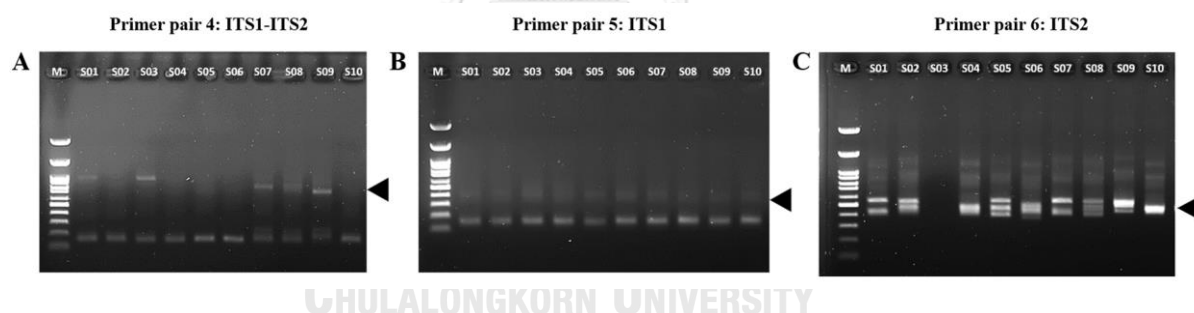


Figure 19: The 1% agarose gel electrophoresis for comparisons among 3 primer pairs specific to fungal ITS PCR products

(A) The full-length ITS amplified products from primer pair 4 (ITS_1F/ITS_4R). (B) The partial ITS1 products using primer pair 5 (ITS_1F / ITS_2R). (C) The partial ITS2 amplicons are based on primer pair 6 (ITS_86F/ITS_4R). M: 100 bp ladder marker. S01-S10: representative PDF samples. The triangle indicated the expected band.

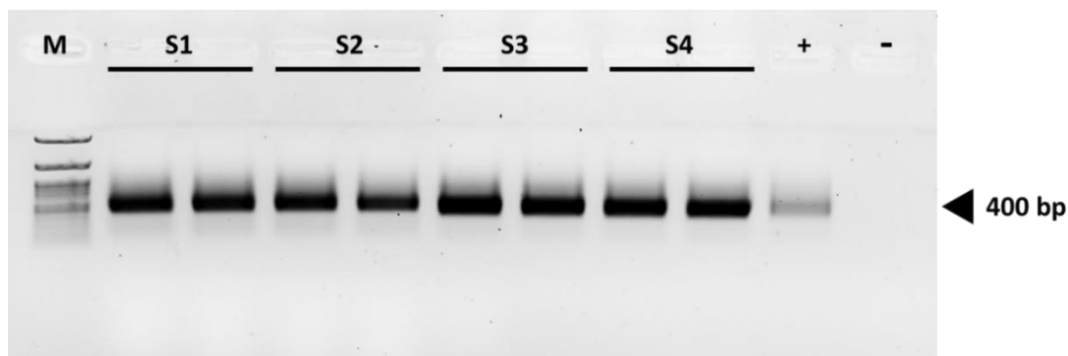


Figure 20: The representative PCR products obtained from the amplification of fungal ITS2 by ITS2_86F/ITS_4R primers

M: 100 bp ladder marker. S1-S4: representative PDE samples. + and – are positive and negative controls, respectively. The triangle indicated the expected band (approximately 400 bp).

6. Diversity of fungi in peritoneal dialysis effluent

For the ITS2 amplicon sequencing based on the high-throughput ONT platform, a total of 1,272,777 raw sequencing reads were obtained from the 69 PDE samples. These sequences included an average of 18,446 reads per sample. In this study, the average of 10,656 reads per sample can be sufficiently classified the fungal composition patterns (Table 13). The result of the rarefaction curves showed that these sequences had sufficient coverage to accurately classify the fungal diversity (Figure 21). The Chao1 (richness) and Shannon (richness and evenness) indexes were used for the determination of the alpha diversity as summarized in Table 14.

Table 13: Summary of ITS2 sequencing data

Targeted gene	Total raw reads	Average reads/Sample	Average classified reads/Sample
ITS2	1,272,777	18,446 ± 11,329	13,537 ± 8,143

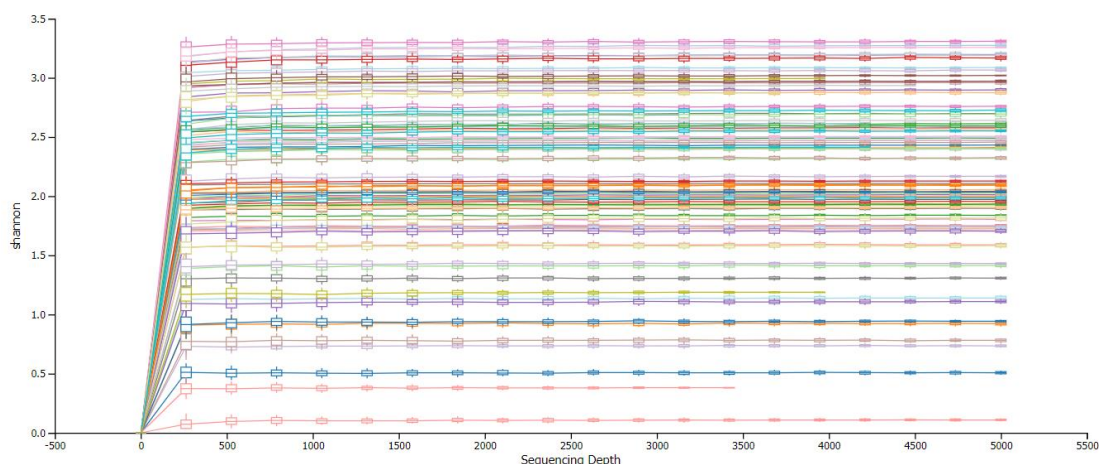


Figure 21: The rarefaction analysis of ITS2

Rarefaction curves demonstrated the sequencing depth for estimation of the Shannon diversity index in each saturated plateau as represented by different colors.

Table 14: Alpha diversity indexes (Chao1 and Shannon) of fungi

Targeted gene	Chao1 index	Shannon index
ITS2	36.59 ± 16.17	2.22 0.06

7. The relative abundance of fungal classification

From the result, the major identified phyla from 69 PDE samples were Basidiomycota followed by Ascomycota and Glomeromycota, respectively, as shown in Figure 22. The most common fungal genera were *Wallemia* followed by *Cladosporium* and *Meyerozyma*, respectively (Figure 23). All subjects were separated into 8 clusters based on the fungal taxonomy patterns in the samples (Figure 24). Heatmap clustering showed that *Cryptococcus* was a unique fungal community in Cluster 1. In addition, the dominant fungal abundance included *Sterigmatomyces* (Cluster 2), *Exobasidium* and *Meyerozyma* (Cluster 3) and *Cladosporium* (Cluster 4). Interestingly, *Wallemia* were clustered according to the percentage of relative abundance by greater than 40% but less than 70% (Cluster 5-7) and greater than 70% (Cluster 8). Cluster 6 and Cluster 7 were distinguished by co-dominant *Wallemia* with *Meyerozyma* and *Cladosporium*, respectively.

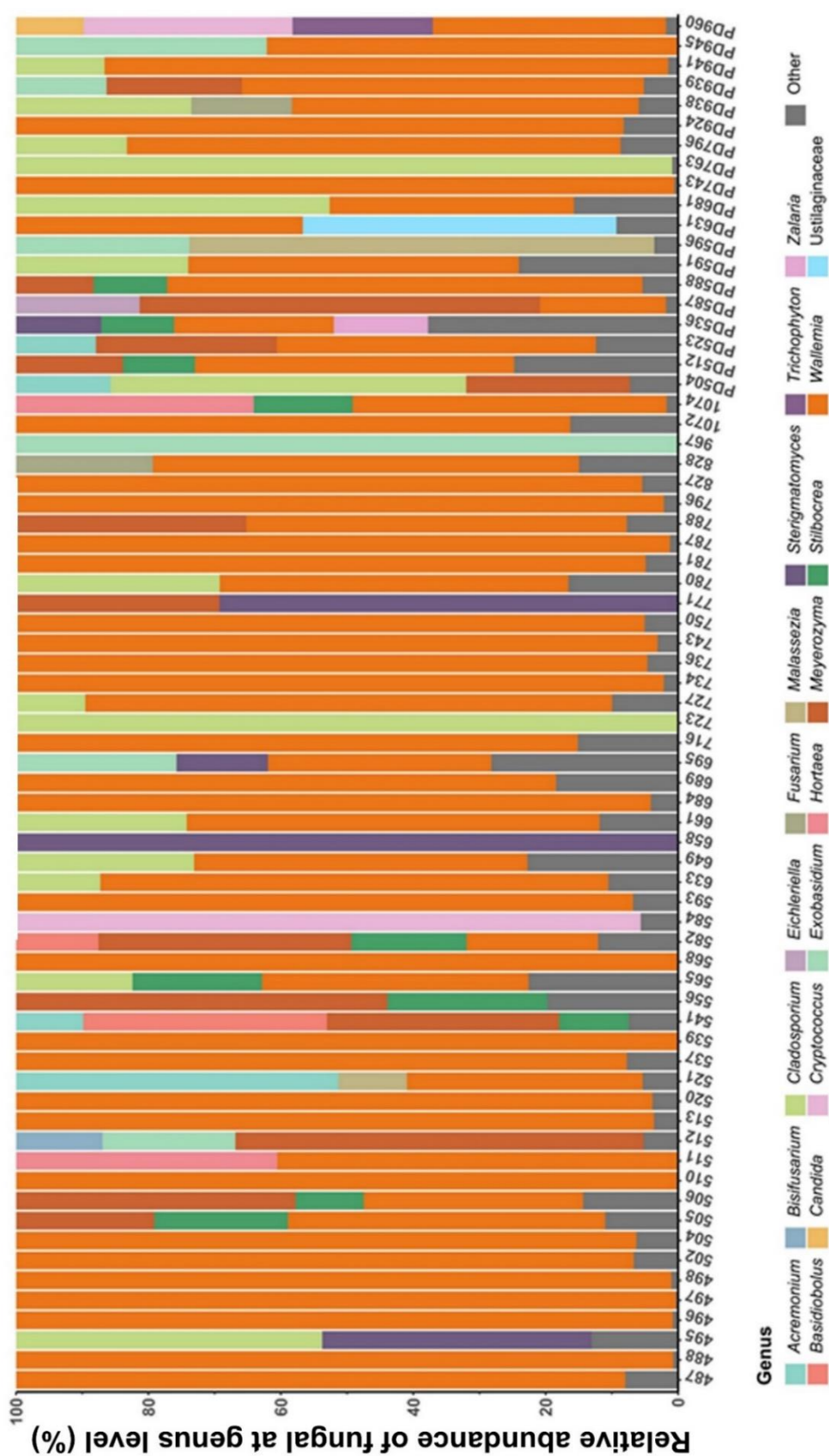


Figure 23: The taxonomic classification of fungal genera in 69 PDE samples
The colored bars represent the different fungal genera.

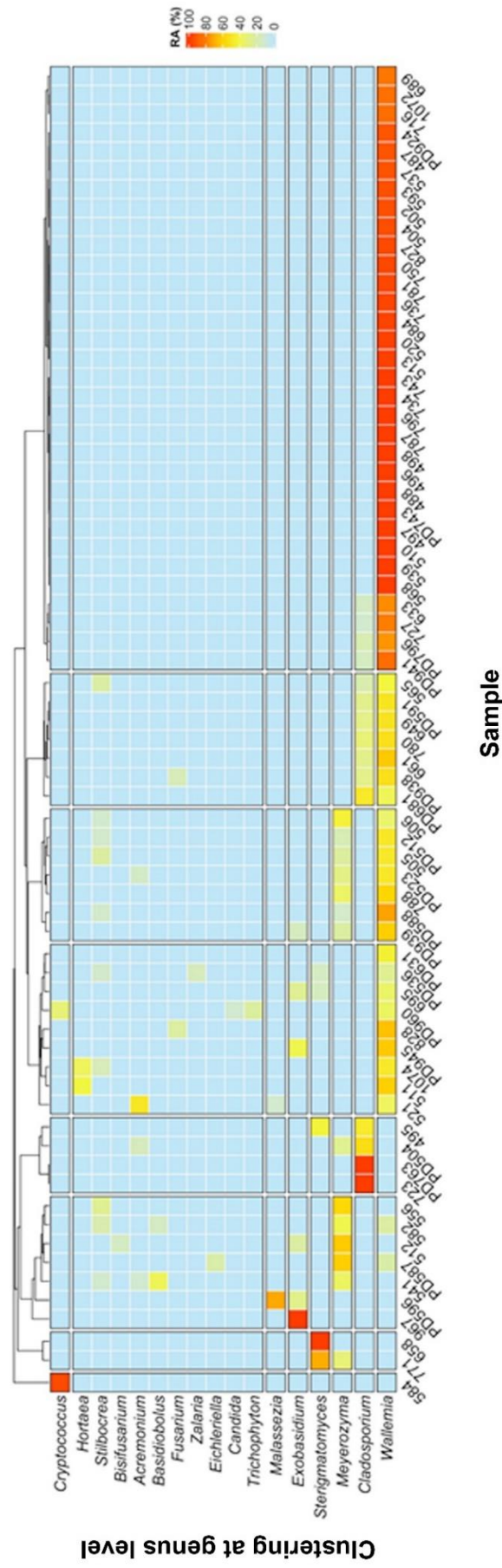


Figure 24: Heatmap visualized the hierarchical clustering of the fungal taxonomy in each sample based on genus level.
The color represented the relative abundance (RA) of percentage (%) for fungal genera.

8. Fungal identification through the metagenomic approaches

High-throughput ITS2 sequencing can be used for fungal classification in PDE samples. There were 66.35% (69/104 samples) positive for fungus obtained from metagenomic results. *Wallemia* was the most fungal genera found in the samples. Interestingly, in this study was observed co-dominance of the highest abundances of fungi in 5 samples. The results showed that the abundant fungi were dominated by *Wallemia* and order Hypocreales in Samples PD512 and PD523. *Wallemia* and phylum Ascomycota co-dominated in Sample 506 whereas order Hypocreales and class Agaricomycetes co-dominated in Sample 495. Furthermore, Sample 556 was multi-dominated by *Ascomycota* sp., order Hypocreales, and phylum Ascomycota as summarized in Table 15.



Table 15: Summary of fungal identification through the metagenomic approaches

Fungal identification	Sample ID	Number of cases (%)
Agaricomycetes	967	1/69 (1.45%)
Ascomycota	537, 565, 723, PD938, PD960	5/69 (7.25%)
Hypocreales	512, 541, PD504, PD536, PD763	5/69 (7.25%)
Hypocreales, Agaricomycetes	495	1/69 (1.45%)
Hypocreales, Ascomycota, <i>Ascomycota</i> sp	556	1/69 (1.45%)
Hypocreales, <i>Wallemia</i>	PD512, PD523	2/69 (2.90%)
<i>Malassezia</i> sp	PD596	1/69 (1.45%)
<i>Sterigmatomyces halophilus</i>	658, 771	2/69 (2.90%)
Tremellomycetes	584	1/69 (1.45%)
<i>Wallemia</i>	487, 488, 496, 497, 498, 502, 504, 505, 510, 511, 513, 520, 521, 539, 568, 582, 593, 633, 649, 661, 684, 689, 695, 716, 727, 734, 736, 743, 750, 780, 781, 787, 788, 796, 827, 828, 1072, 1074, PD587, PD588, PD591, PD631, PD681, PD743, PD796, PD924, PD939, PD941, PD945	49/69 (71.01%)
<i>Wallemia</i> , Ascomycota	506	1/69 (1.45%)

CHAPTER V

DISCUSSION AND CONCLUSION

Amplicon sequencing through the ONT platform is a powerful strategy for microbial classification and has been popularly employed for microbiome analysis from diverse human clinical samples (65). This sequencing platform is a culture-free method that provides a cost-effective technique and essential benefits regarding long-read data (66). The amplification and sequencing of the full-length 16S rDNA gene (approximately 1,500 bp) and ITS region (including 5.8S rDNA gene, approximately 800 bp) can allow bacterial and fungal identification up to species level with high accuracy and sensitivity (67, 68). However, a good-quality DNA sample was required to amplify the full-length gene for long reads sequencing. Therefore, the limitation of this approach is the difficulty of full-length gene amplification in the samples with low-quality DNA.

In the present study, the DNA in PDE samples was degraded due to several reasons including being collected without nucleic acid preservation (NAP) buffer, multiple freeze-thaw, and kept at -20 °C for a long period (69). Degraded samples may have insufficient quantities of DNA to amplify the full-length 16S rDNA gene and ITS region. Therefore, the partial gene of the 16S rDNA gene (V1-V4 regions) and ITS2 region amplification was applied for bacteria and fungi, respectively. For further study, the sample should be preserved in NAP buffer (70), and avoiding multiple freeze-thaw would be more appropriate for the full-length amplicon sequencing.

Another reason may be lysis buffer in the DNA extraction process. Since a cell wall can be found in the majority of bacteria and fungi and is substantially harder than the plasma membrane of mammalian cells. A mild lysis buffer can be used to selectively lyse the plasma membrane without damaging the microorganisms. However, some microorganisms are more likely to be destroyed by a selective lysis buffer which leads to a low quantity of DNA for the library preparation and sequencing (71).

For bacterial identification, this study showed that the traditional bacterial culture method provides positive results in only 56 among 104 samples (53.8%) whereas the 16S rDNA metagenomic approach can identify up to 89 samples (85.6%). Moreover, our study showed that 42/56 samples (75%) had the same results between the traditional culture method and 16S rDNA sequencing. Noticeably, 33 samples (31.73%) without traditional culture results can be classified the bacterial species through 16S rDNA amplicon sequencing. The result obtained from this study was comparable to a recent study that performed shotgun metagenomic analysis to identify pathogens in PDE samples based on the BGISEQ platforms as summarized in Table 16 (72).

Table 16: The comparison of positive rate from bacterial culture and metagenomic analysis between our study and recent report

Result	Our study	Recent study
Positive rate from culture method	56/104 (53.85%)	18/30 (60%)
Positive rate from metagenomic analysis	89/104 (85.58%)	26/30 (86.67%)
Positive rate from both techniques	56/104 (53.85%)	15/30 (50%)
Negative rate from both techniques	0/104 (0%)	1/30 (3.33%)

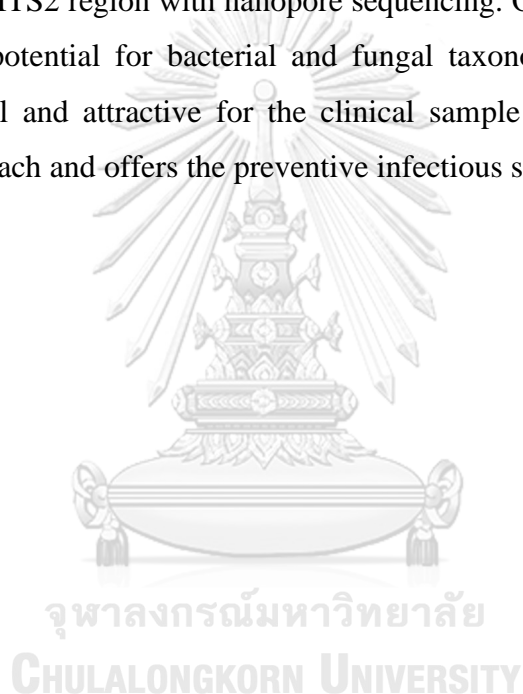
The accurate and precise identification of fungi is challenging in the traditional culture method as it is not routine for clinical examination. The traditional fungal culture method provides positive results in only 13/104 samples (12.5%) whereas ITS2 nanopore sequencing contributed positive results in 69/104 samples (66.3%). Interestingly, 56/69 samples (81.2%) negative for traditional culture can be classified in the fungal taxonomy through metagenomic analysis, indicating that the metagenomic approach had a higher potential for microbial classification than the traditional culture method. However, some samples cannot be classified by the metagenomic approach because DNA yields in PDE samples might be severely degraded during long-term storage.

In this study, the 16S rDNA gene sequencing result showed that Firmicutes, Proteobacteria, and Actinobacteria were the dominant phylum in ESKD patients similar to the previous study (73). In line with our findings, previous studies discovered microbiomes in the peritoneal tissue of ESKD patients harbor a high abundance of Firmicutes and Proteobacteria (5). At the species level, the dominance of *Escherichia coli*, *Phyllobacterium myrsinacearum*, *Streptococcus gallolyticus*, *Staphylococcus epidermidis*, and *Shewanella algae* in the PDE samples could be the clinical importance. The bacterial genera *Escherichia*, *Streptococcus*, and *Staphylococcus* were also detected by traditional culture and shotgun metagenomic analysis in a recent study (72). Another study revealed the causative microorganisms in PDE samples based on traditional culture and found both gram-positive bacteria (i.e., *Staphylococcus*, *Streptococcus*, *Enterococcus*) and gram-negative bacteria (i.e., *Escherichia*, *Klebsiella*, *Pseudomonas*) which are partially consistent to our study (74).

Generally, *E. coli* is a frequent gram-negative peritonitis bacterium and can be produced the extended-spectrum β -lactamase (ESBL) associated with a poorer prognosis (75). Interestingly, PD-related peritonitis caused by *Streptococcus sp.* was reported from the entry routes into the peritoneal cavity including contamination during the exchange procedure, bacterial translocation, hematological dissemination with oral and dental procedures, and catheter-related process (76). More studies have shown that the most common pathogens are coagulase-negative staphylococcal species, including *Staphylococcus epidermidis* and *Staphylococcus aureus* which commonly colonize human skin and hands and may also lead to peritonitis when exit-site and tunnel infections (77, 78). *Shewanella sp.* is hydrogen sulfide-producing motile gram-negative bacilli. The common clinical syndromes are skin and soft tissue infections, including peritoneal catheter-associated infections (79). Finally, *Phyllobacterium myrsinacearum* is a gram-negative bacterium that causes infections in humans. Due to *Phyllobacterium myrsinacearum* cannot grow on standard media culture, the identification of this bacteria based on a metagenomic approach raised several outstanding questions about whether it can cause human severe infection (80).

Based on the ITS2 sequencing result, we found *Wallemia* at the genus level is the most dominant fungi in the PDE samples. The Basidiomycota genus *Wallemia* has been classified as a minor component with potential functional significance within the human gut microbiota (81). Moreover, a few studies have reported that *Wallemia sp.* be related to human health problems such as allergological conditions or rare subcutaneous/cutaneous infections (82).

In conclusion, our study demonstrated the metagenomic analysis of the low abundance DNA extracted from PDE samples based on the partial gene amplification of 16S rDNA and ITS2 region with nanopore sequencing. Our metagenomic approach provided a high potential for bacterial and fungal taxonomic classification, which would be practical and attractive for the clinical sample as an alternative culture-independent approach and offers the preventive infectious strategy in CDK patients.



REFERENCES

1. Akchurin OM. Chronic Kidney Disease and Dietary Measures to Improve Outcomes. *Pediatr Clin North Am.* 2019;66(1):247-67.
2. National Institute of Diabetes and Digestive and Kidney Diseases (NIDDK) [Internet]. Peritoneal Dialysis 1950 [updated January 2018]. Available from: <https://www.niddk.nih.gov/health-information/kidney-disease/kidney-failure/peritoneal-dialysis>.
3. Zimmerman AM. Peritoneal dialysis: increasing global utilization as an option for renal replacement therapy. *J Glob Health.* 2019;9(2):020316.
4. Akoh JA. Peritoneal dialysis associated infections: An update on diagnosis and management. *World J Nephrol.* 2012;1(4):106-22.
5. Simoes-Silva L, Araujo R, Pestana M, Soares-Silva I, Sampaio-Maia B. Peritoneal Microbiome in End-Stage Renal Disease Patients and the Impact of Peritoneal Dialysis Therapy. *Microorganisms.* 2020;8(2).
6. Golper TA, Brier ME, Bunke M, Schreiber MJ, Bartlett DK, Hamilton RW, et al. Risk factors for peritonitis in long-term peritoneal dialysis: the Network 9 peritonitis and catheter survival studies. Academic Subcommittee of the Steering Committee of the Network 9 Peritonitis and Catheter Survival Studies. *Am J Kidney Dis.* 1996;28(3):428-36.
7. Coward RA, Gokal R, Wise M, Mallick NP, Warrell D. Peritonitis associated with vaginal leakage of dialysis fluid in continuous ambulatory peritoneal dialysis. *Br Med J (Clin Res Ed).* 1982;284(6328):1529.
8. Vaziri ND, Goshtasbi N, Yuan J, Jellbauer S, Moradi H, Raffatellu M, et al. Uremic plasma impairs barrier function and depletes the tight junction protein constituents of intestinal epithelium. *Am J Nephrol.* 2012;36(5):438-43.
9. Vaziri ND, Yuan J, Norris K. Role of urea in intestinal barrier dysfunction and disruption of epithelial tight junction in chronic kidney disease. *Am J Nephrol.* 2013;37(1):1-6.
10. Deng X, Achari A, Federman S, Yu G, Somasekar S, Bartolo I, et al. Metagenomic sequencing with spiked primer enrichment for viral diagnostics and genomic surveillance. *Nat Microbiol.* 2020;5(3):443-54.

11. Simner PJ, Miller S, Carroll KC. Understanding the Promises and Hurdles of Metagenomic Next-Generation Sequencing as a Diagnostic Tool for Infectious Diseases. *Clin Infect Dis*. 2018;66(5):778-88.
12. Chiu CY. Viral pathogen discovery. *Curr Opin Microbiol*. 2013;16(4):468-78.
13. Gu W, Deng X, Lee M, Sucu YD, Arevalo S, Stryke D, et al. Rapid pathogen detection by metagenomic next-generation sequencing of infected body fluids. *Nat Med*. 2021;27(1):115-24.
14. Greninger AL, Naccache SN, Federman S, Yu G, Mbala P, Bres V, et al. Rapid metagenomic identification of viral pathogens in clinical samples by real-time nanopore sequencing analysis. *Genome Med*. 2015;7:99.
15. Qiu C, Huang S, Park J, Park Y, Ko YA, Seasock MJ, et al. Renal compartment-specific genetic variation analyses identify new pathways in chronic kidney disease. *Nat Med*. 2018;24(11):1721-31.
16. Levey AS, Atkins R, Coresh J, Cohen EP, Collins AJ, Eckardt KU, et al. Chronic kidney disease as a global public health problem: approaches and initiatives - a position statement from Kidney Disease Improving Global Outcomes. *Kidney Int*. 2007;72(3):247-59.
17. Chambers JC, Zhang W, Lord GM, van der Harst P, Lawlor DA, Sehmi JS, et al. Genetic loci influencing kidney function and chronic kidney disease. *Nat Genet*. 2010;42(5):373-5.
18. National Institute of Diabetes and Digestive and Kidney Diseases (NIDDK) [Internet]. Chronic Kidney Disease (CKD) 2016 [updated October 2016]. Available from: <https://www.niddk.nih.gov/health-information/kidney-disease/chronic-kidney-disease-ckd/all-content>.
19. Centers for Disease Control and Prevention (CDC) [Internet]. Chronic kidney disease basics 2021. Available from: <https://www.cdc.gov/kidneydisease/basics.html>.
20. American Kidney Fund 2021 [Internet]. [updated October 26, 2022]. Available from: <https://www.kidneyfund.org/kidney-disease/chronic-kidney-disease-ckd/stages-of-chronic-kidney-disease/>.
21. National Kidney Foundation [Internet]. Estimated Glomerular Filtration Rate (eGFR) 2021 [updated September 23, 2021]. Available from:

<https://www.kidney.org/atoz/content/gfr>.

22. National Kidney Foundation [Internet]. Kidney Transplant 2021 [updated April 08, 2021]. Available from: <https://www.kidney.org/atoz/content/kidney-transplant>.
23. Perl J, Davies SJ, Lambie M, Pisoni RL, McCullough K, Johnson DW, et al. The Peritoneal Dialysis Outcomes and Practice Patterns Study (PDOPPS): Unifying Efforts to Inform Practice and Improve Global Outcomes in Peritoneal Dialysis. *Perit Dial Int*. 2016;36(3):297-307.
24. InformedHealth.org [Internet]. Cologne, Germany: Institute for Quality and Efficiency in Health Care; 2006-. How does dialysis work? 2018 Mar 8. Available from: <https://www.ncbi.nlm.nih.gov/books/NBK492981>.
25. Oki R, Tsuji S, Hamasaki Y, Komaru Y, Miyamoto Y, Matsuura R, et al. Time until treatment initiation is associated with catheter survival in peritoneal dialysis-related peritonitis. *Sci Rep*. 2021;11(1):6547.
26. Rubin HR, Fink NE, Plantinga LC, Sadler JH, Klinger AS, Powe NR. Patient ratings of dialysis care with peritoneal dialysis vs hemodialysis. *JAMA*. 2004;291(6):697-703.
27. Moist LM, Port FK, Orzol SM, Young EW, Ostbye T, Wolfe RA, et al. Predictors of loss of residual renal function among new dialysis patients. *J Am Soc Nephrol*. 2000;11(3):556-64.
28. Jansen MA, Hart AA, Korevaar JC, Dekker FW, Boeschoten EW, Krediet RT, et al. Predictors of the rate of decline of residual renal function in incident dialysis patients. *Kidney Int*. 2002;62(3):1046-53.
29. Lysaght MJ, Vonesh EF, Gotch F, Ibels L, Keen M, Lindholm B, et al. The influence of dialysis treatment modality on the decline of remaining renal function. *ASAIO Trans*. 1991;37(4):598-604.
30. Didelot X, Bowden R, Wilson DJ, Peto TEA, Crook DW. Transforming clinical microbiology with bacterial genome sequencing. *Nat Rev Genet*. 2012;13(9):601-12.
31. Hilton SK, Castro-Nallar E, Perez-Losada M, Toma I, McCaffrey TA, Hoffman EP, et al. Metataxonomic and Metagenomic Approaches vs. Culture-Based Techniques for Clinical Pathology. *Front Microbiol*. 2016;7:484.
32. Wang B, Xu JS, Wang CX, Mi ZH, Pu YP, Hui M, et al. Antimicrobial

susceptibility of *Neisseria gonorrhoeae* isolated in Jiangsu Province, China, with a focus on fluoroquinolone resistance. *J Med Microbiol*. 2006;55(Pt 9):1251-5.

33. Intergrate DNA Technologies [Internet]. Amplicon sequencing. Available from: <https://sg.idtdna.com/pages/technology/next-generation-sequencing/dna-sequencing/targeted-sequencing/amplicon-sequencing>.

34. Klindworth A, Pruesse E, Schweer T, Peplies J, Quast C, Horn M, et al. Evaluation of general 16S ribosomal RNA gene PCR primers for classical and next-generation sequencing-based diversity studies. *Nucleic Acids Res*. 2013;41(1):e1.

35. Microbiome Insights [Internet]. 16S rRNA Gene Sequencing vs. Shotgun Metagenomic Sequencing: Microbiome Insights; [updated 2020]. Available from: <https://blog.microbiomeinsights.com/16s-rna-sequencing-vs-shotgun-metagenomic-sequencing>.

36. Forbes JD, Knox NC, Ronholm J, Pagotto F, Reimer A. Metagenomics: The Next Culture-Independent Game Changer. *Front Microbiol*. 2017;8:1069.

37. Kuczynski J, Lauber CL, Walters WA, Parfrey LW, Clemente JC, Gevers D, et al. Experimental and analytical tools for studying the human microbiome. *Nat Rev Genet*. 2011;13(1):47-58.

38. Dunne WM, Jr., Westblade LF, Ford B. Next-generation and whole-genome sequencing in the diagnostic clinical microbiology laboratory. *Eur J Clin Microbiol Infect Dis*. 2012;31(8):1719-26.

39. Perez-Losada M, Castro-Nallar E, Bendall ML, Freishtat RJ, Crandall KA. Dual Transcriptomic Profiling of Host and Microbiota during Health and Disease in Pediatric Asthma. *PLoS One*. 2015;10(6):e0131819.

40. Fukuda K, Ogawa M, Taniguchi H, Saito M. Molecular Approaches to Studying Microbial Communities: Targeting the 16S Ribosomal RNA Gene. *J UOEH*. 2016;38(3):223-32.

41. Mincheol Kim JC. *Methods in Microbiology: Elsevier*; 2014 2014.

42. CD Genomics [Internet]. 18S rRNA and Its Use in Fungal Diversity Analysis [updated 2018]. Available from: <https://www.cd-genomics.com/blog/18s-rna-and-its-use-in-fungal-diversity-analysis/>.

43. Villalobos G, Orozco-Mosqueda GE, Lopez-Perez M, Lopez-Escamilla E,

- Cordoba-Aguilar A, Rangel-Gamboa L, et al. Suitability of internal transcribed spacers (ITS) as markers for the population genetic structure of *Blastocystis* spp. *Parasit Vectors*. 2014;7:461.
44. Hribova E, Cizkova J, Christelova P, Taudien S, de Langhe E, Dolezel J. The ITS1-5.8S-ITS2 sequence region in the Musaceae: structure, diversity and use in molecular phylogeny. *PLoS One*. 2011;6(3):e17863.
 45. Eickbush TH, Eickbush DG. Finely orchestrated movements: evolution of the ribosomal RNA genes. *Genetics*. 2007;175(2):477-85.
 46. Bromberg JS, Fricke WF, Brinkman CC, Simon T, Mongodin EF. Microbiota-implications for immunity and transplantation. *Nat Rev Nephrol*. 2015;11(6):342-53.
 47. Liu J, Yu Y, Cai Z, Bartlam M, Wang Y. Comparison of ITS and 18S rDNA for estimating fungal diversity using PCR-DGGE. *World J Microbiol Biotechnol*. 2015;31(9):1387-95.
 48. Amarasinghe SL, Su S, Dong X, Zappia L, Ritchie ME, Gouil Q. Opportunities and challenges in long-read sequencing data analysis. *Genome Biol*. 2020;21(1):30.
 49. Martin O Pollard DG, Alexander J Mentzer, Tarryn Porter, Manjinder S Sandhu. Long reads: their purpose and place 2018 August 01, 2018.
 50. Yuan Y, Bayer PE, Batley J, Edwards D. Improvements in Genomic Technologies: Application to Crop Genomics. *Trends Biotechnol*. 2017;35(6):547-58.
 51. Slatko BE, Gardner AF, Ausubel FM. Overview of Next-Generation Sequencing Technologies. *Curr Protoc Mol Biol*. 2018;122(1):e59.
 52. Jain M, Olsen HE, Paten B, Akeson M. The Oxford Nanopore MinION: delivery of nanopore sequencing to the genomics community. *Genome Biol*. 2016;17(1):239.
 53. Cao MD, Ganesamoorthy D, Elliott AG, Zhang H, Cooper MA, Coin LJ. Streaming algorithms for identification of pathogens and antibiotic resistance potential from real-time MinION(TM) sequencing. *Gigascience*. 2016;5(1):32.
 54. Sutton MA, Burton AS, Zaikova E, Sutton RE, Brinckerhoff WB, Bevilacqua JG, et al. Radiation Tolerance of Nanopore Sequencing Technology for Life Detection on Mars and Europa. *Sci Rep*. 2019;9(1):5370.
 55. MIT Technology Review [Internet]. Nanopore sequencing [updated 2012]. Available from: <https://www.technologyreview.com/technology/nanopore-sequencing/>.

56. Bhattaru SAT, Jacopo Saboda, Kendall Borowsky, Jonathan Ruvkun, Gary Zuber, Maria T. Carr, Christopher E. Development of a Nucleic Acid-Based Life Detection Instrument Testbed. March, 2019 *IEEE*; 2019. p. 8742193.
57. Kanjanabuch T, Puapatanakul P, Halue G, Lorrvinittun P, Tangjittong K, Pongpirul K, et al. Implementation of PDOPPS in a middle-income country: Early lessons from Thailand. *Perit Dial Int*. 2022;42(1):83-91.
58. Wick RR, Judd LM, Holt KE. Performance of neural network basecalling tools for Oxford Nanopore sequencing. *Genome Biol*. 2019;20(1):129.
59. Lanfear R, Schalamun M, Kainer D, Wang W, Schwessinger B. MinIONQC: fast and simple quality control for MinION sequencing data. *Bioinformatics*. 2019;35(3):523-5.
60. Rodriguez-Perez H, Ciuffreda L, Flores C. NanoCLUST: a species-level analysis of 16S rRNA nanopore sequencing data. *Bioinformatics*. 2021;37(11):1600-1.
61. Cole JR, Chai B, Marsh TL, Farris RJ, Wang Q, Kulam SA, et al. The Ribosomal Database Project (RDP-II): previewing a new autoaligner that allows regular updates and the new prokaryotic taxonomy. *Nucleic Acids Res*. 2003;31(1):442-3.
62. Bolyen E, Rideout JR, Dillon MR, Bokulich NA, Abnet CC, Al-Ghalith GA, et al. Reproducible, interactive, scalable and extensible microbiome data science using QIIME 2. *Nat Biotechnol*. 2019;37(8):852-7.
63. Edgar RC, Haas BJ, Clemente JC, Quince C, Knight R. UCHIME improves sensitivity and speed of chimera detection. *Bioinformatics*. 2011;27(16):2194-200.
64. Rognes T, Flouri T, Nichols B, Quince C, Mahe F. VSEARCH: a versatile open source tool for metagenomics. *PeerJ*. 2016;4:e2584.
65. Fu Y, Chen Q, Xiong M, Zhao J, Shen S, Chen L, et al. Clinical Performance of Nanopore Targeted Sequencing for Diagnosing Infectious Diseases. *Microbiol Spectr*. 2022;10(2):e0027022.
66. Midha MK, Wu M, Chiu KP. Long-read sequencing in deciphering human genetics to a greater depth. *Hum Genet*. 2019;138(11-12):1201-15.
67. Matsuo Y, Komiya S, Yasumizu Y, Yasuoka Y, Mizushima K, Takagi T, et al. Full-length 16S rRNA gene amplicon analysis of human gut microbiota using MinION nanopore sequencing confers species-level resolution. *BMC Microbiol*. 2021;21(1):35.

68. D'Andreano S, Cusco A, Francino O. Rapid and real-time identification of fungi up to species level with long amplicon nanopore sequencing from clinical samples. *Biol Methods Protoc.* 2021;6(1):bpaa026.
69. Monger XC, Saucier L, Gilbert AA, Vincent AT. Stabilization of swine faecal samples influences taxonomic and functional results in microbiome analyses. *MethodsX.* 2022;9:101716.
70. Menke S, Gillingham MA, Wilhelm K, Sommer S. Home-Made Cost Effective Preservation Buffer Is a Better Alternative to Commercial Preservation Methods for Microbiome Research. *Front Microbiol.* 2017;8:102.
71. Shi Y, Wang G, Lau HC, Yu J. Metagenomic Sequencing for Microbial DNA in Human Samples: Emerging Technological Advances. *Int J Mol Sci.* 2022;23(4).
72. Ye P, Xie C, Wu C, Yu C, Chen Y, Liang Z, et al. The application of metagenomic next-generation sequencing for detection of pathogens from dialysis effluent in peritoneal dialysis-associated peritonitis. *Perit Dial Int.* 2022;42(6):585-90.
73. Vaziri ND, Wong J, Pahl M, Piceno YM, Yuan J, DeSantis TZ, et al. Chronic kidney disease alters intestinal microbial flora. *Kidney Int.* 2013;83(2):308-15.
74. Dzekova-Vidimliski P, Nikolov IG, Gjorgjievski N, Selim G, Trajceska L, Stojanoska A, et al. Peritoneal Dialysis-Related Peritonitis: Rate, Clinical Outcomes and Patient Survival. *Pril (Makedon Akad Nauk Umet Odd Med Nauki).* 2021;42(3):47-55.
75. Feng X, Yang X, Yi C, Guo Q, Mao H, Jiang Z, et al. Escherichia coli Peritonitis in peritoneal dialysis: the prevalence, antibiotic resistance and clinical outcomes in a South China dialysis center. *Perit Dial Int.* 2014;34(3):308-16.
76. Chao CT, Lee SY, Yang WS, Chen HW, Fang CC, Yen CJ, et al. Viridans streptococci in peritoneal dialysis peritonitis: clinical courses and long-term outcomes. *Perit Dial Int.* 2015;35(3):333-41.
77. Salzer WL. Peritoneal dialysis-related peritonitis: challenges and solutions. *Int J Nephrol Renovasc Dis.* 2018;11:173-86.
78. Gadola L, Poggi C, Dominguez P, Poggio MV, Lungo E, Cardozo C. Risk Factors And Prevention of Peritoneal Dialysis-Related Peritonitis. *Perit Dial Int.* 2019;39(2):119-25.
79. Yan Y, Chai X, Chen Y, Zhang X. The Fulminating Course of Infection Caused

by *Shewanella* algae: A Case Report. *Infect Drug Resist.* 2022;15:1645-50.

80. Gareth Hughes CP, Swarupsinh Chavdab, Miruna D.Davida. The first case report of human infection with *Phyllobacterium myrsinacearum* causing spondylodiscitis. *Clinical Infection in Practice.* 2020.

81. Liguori G, Lamas B, Richard ML, Brandi G, da Costa G, Hoffmann TW, et al. Fungal Dysbiosis in Mucosa-associated Microbiota of Crohn's Disease Patients. *J Crohns Colitis.* 2016;10(3):296-305.

82. Zajc J, Gunde-Cimerman N. The Genus *Wallemia*-From Contamination of Food to Health Threat. *Microorganisms.* 2018;6(2).



VITA

NAME	Suthida Visedthorn
DATE OF BIRTH	31 October 1997
PLACE OF BIRTH	Bangkok, Thailand
INSTITUTIONS ATTENDED	Bachelor's degree of science, Bioscience and Technology (International Program), Kasetsart University.
HOME ADDRESS	7/1013, Liap Khlong Song 19 Alley, Sam Wa Tawan Tok, Khlong Sam Wa, Bangkok 10510, Thailand.

